

¹ **Title:** Carbon cycling in mature and regrowth forests globally: a macroecological synthesis based on the
² global Forest Carbon (ForC) database

³ **Authors:**

⁴ Kristina J. Anderson-Teixeira^{1,2*}

⁵ Valentine Herrmann¹

⁶ Becky Banbury Morgan³

⁷ Ben Bond-Lamberty⁴

⁸ Susan C. Cook-Patton⁵

⁹ Abigail E. Ferson^{1,6}

¹⁰ Jennifer C. McGarvey¹

¹¹ Helene C. Muller-Landau¹

¹² Maria M. H. Wang^{1,7}

¹³ **Author Affiliations:**

¹⁴ 1. Conservation Ecology Center; Smithsonian Conservation Biology Institute; National Zoological Park,
¹⁵ Front Royal, VA 22630, USA

¹⁶ 2. Center for Tropical Forest Science-Forest Global Earth Observatory; Smithsonian Tropical Research
¹⁷ Institute; Panama, Republic of Panama

¹⁸ 3. School of Geography, University of Leeds, Leeds, UK

¹⁹ 4. Joint Global Change Research Institute, Pacific Northwest National Laboratory, College Park
²⁰ Maryland 20740, USA

²¹ 5. The Nature Conservancy; Arlington VA 22203, USA

²² 6. College of Natural Resources, University of Idaho; Moscow, Idaho 83843, USA

²³ 7. Grantham Centre for Sustainable Futures and Department of Animal and Plant Sciences, University of
²⁴ Sheffield, Western Bank, Sheffield, South Yorkshire S10 2TN, UK

²⁵ *corresponding author: teixeirak@si.edu; +1 540 635 6546

²⁶ ## [1] 0

²⁷ **NOTES TO COAUTHORS:**

- ²⁸ • “???” indicates a reference that we have entered in the .Rmd file, but not yet in the bibliography file.
²⁹ Don’t worry about those. (However, places with “REF” need references)
³⁰ • bold/ italic text indicates places where I know we need to go back and revisit/ fill in info

31 Summary

32 Background. Earth's climate is closely linked to forests, which strongly influence atmospheric carbon dioxide
33 (CO_2) and climate by their impact on the global carbon (C) cycle. However, efforts to incorporate forests
34 into climate models and CO_2 accounting frameworks have been constrained by a lack of accessible,
35 global-scale data on how C cycling varies across forest types and stand ages.

36 Methods/Design. Here, we draw from the Global Forest Carbon Database, ForC, to provide a macroscopic
37 overview of C cycling in the world's forests, giving special attention to stand age-related variation.

38 Specifically, we use 12124 *ForC* records from 869 geographic locations representing 34 C cycle variables to
39 characterize ensemble C budgets for four broad forest types (tropical broadleaf evergreen, temperate
40 broadleaf, temperate conifer, and taiga), including estimates for both mature and regrowth (age <100 years)
41 forests. For regrowth forests, we quantify age trends for all variables.

42 Review Results/ Synthesis. *ForC v3.0* yielded a fairly comprehensive picture of C cycling in the world's
43 major forest biomes, with broad closure of C budgets. The rate of C cycling generally increased from boreal
44 to tropical regions in both mature and regrowth forests, whereas C stocks showed less directional variation.
45 The majority of flux variables, together with most live biomass pools, increased significantly with stand age,
46 and the rate of increase again tended to increase from boreal to tropical regions.

47 Discussion. NEED TO WRITE THIS!!!

48 Key words: forest ecosystems; carbon cycle; stand age; productivity; respiration; biomass; global

49 **Background**

50 Forest ecosystems are shaping the course of climate change (IPCC1.5) through their influence on atmospheric
51 carbon dioxide (CO₂). Despite the centrality of forest C cycling in regulating atmospheric CO₂, important
52 uncertainties in climate models (???, ???, ???, Krause *et al* 2018) and CO₂ accounting frameworks (Pan *et*
53 *al* 2011) can be traced to lack of accessible, comprehensive data on how C cycling varies across forest types
54 and in relation to stand history. These require large-scale databases with global coverage, which runs
55 contrary to the nature in which forest C stocks and fluxes are measured and published. While remote sensing
56 measurements are increasingly useful for global- or regional-scale estimates of a few critical variables [e.g.,
57 aboveground biomass: (???); **REF**; gross primary productivity, *GPP*: Li and Xiao (2019); **REFS for**
58 **biomass change, net CO2 flux**], measurement of most forest C stocks and fluxes require intensive
59 on-the-ground data collection. Here, we provide a robust and comprehensive analysis of carbon cycling from
60 a stand to global level, and by biome and stand age, using the largest global compilation of forest carbon
61 data, which is available in our open source Global Carbon Forest database (ForC; Fig. 1).

62 A robust understanding of forest impacts on global C cycling is essential. Annual gross CO₂ sequestration in
63 forests (gross primary productivity, *GPP*) is estimated at >69 Gt C yr⁻¹ (???), or >7 times average annual
64 fossil fuel emissions from 2009-2018 (9.5 ± 0.5 Gt C yr⁻¹; ???). Most of this enormous C sequestration is
65 counterbalanced by CO₂ releases to the atmosphere through ecosystem respiration (*R_{eco}*) or fire, with forests
66 globally dominant as sources of both soil respiration (???) and fire emissions (REF). (check if
67 **deforestation statistic below includes natural fire, exclude here if it does.**) In recent years, the
68 remaining CO₂ sink averaged 3.2 ± 0.6 GtC yr⁻¹ from 2009-2018, offsetting 29% of anthropogenic fossil fuel
69 emissions (???). Yet, this sink is reduced by *deforestation/ forest losses to anthropogenic and natural*
70 *disturbances*. Recent net deforestation (*i.e.*, gross deforestation minus regrowth) has been a source of CO₂
71 emissions, estimated at ~1.1 Gt C yr⁻¹ from YEAR-YEAR (Pan *et al* 2011; **UPDATE**), reducing the net
72 forest sink to ~1.1-2.2 Gt C yr⁻¹ across Earth's forests (???).

73 The future of the current forest C sink is dependent both upon forest responses to climate change itself and
74 human land use decisions, which will feedback and strongly influence the course of climate change.
75 Regrowing forests in particular will play an important role (Pugh *et al* 2019), as these represent a large
76 (~#%) and growing proportion of Earth's forests (McDowell *et al* 2020). Understanding, modeling, and
77 managing forest-atmosphere CO₂ exchange is thus central to efforts to mitigate climate change [Grassi *et al*
78 (2017); Griscom *et al* (2017); **Cavaleri et al 2015**].

79 Despite the importance of forests, comprehensive global studies have historically been limited by the scattered
80 and more local nature of research studies. Primary research articles typically cover only a small numbers of
81 sites at a time. The rare exceptions that span regions or continents with rare exceptions spanning regions or
82 continents are typically coordinated through research networks such as ForestGEO (Anderson-Teixeira *et al*
83 2015, e.g., Lutz *et al* 2018) or FLUXNET [Baldocchi *et al* (2001); e.g., **FLUXNET_REF**]. The result of
84 decades of research on forest C cycling is that tens of thousands of records have been distributed across
85 literally thousands of scientific articles –often behind paywalls– along with variation in data formats, units,
86 measurement methods, *etc..* In this format, the data are effectively inaccessible for many global-scale
87 analyses, including those attempting to benchmark model performance with global data (Clark *et al* 2017,
88 Luo *et al* 2012), quantify the the role of forests in the global C cycle (*e.g.*, Pan *et al* 2011), or use
89 book-keeping methods to quantify actual or scenario-based exchanges of CO₂ between forests and the
90 atmosphere [Griscom *et al* (2017); **REFS**]. Scattered data are not conducive for advancing science nor for

making decisions about how to best manage our forests as a tool for constraining the climate crisis.

To address the need for global-scale analyses of forest C cycling, we recently developed *ForC* (Anderson-Teixeira *et al* 2016, pp @anderson-teixeira_forc_2018). *ForC* contains published estimates of forest ecosystem C stocks and annual fluxes (>50 variables), with the different variables capturing the unique ecosystem pools (e.g., woody, foliage, and root biomass; dead wood) and flux types (e.g, gross and net primary productivity; soil, root, and ecosystem respiration). These data are ground-based measurements, and *ForC* contains associated data required for interpretation (e.g., stand history, measurement methods). These data have been amalgamated from original peer-reviewed publications, either directly or via intermediary data compilations. Since its most recent publication (Anderson-Teixeira *et al* 2018), *ForC* has grown to include two additional large databases: the Global Soil Respiration Database (SRDB; Bond-Lamberty and Thomson 2010) and the Global Reforestation Opportunity Assessment database (GROA; Cook-Patton *et al* 2020) that also synthesized published forest C data. Following these additions, *ForC* currently contains 47837 records from 10608 plots and 1532 distinct geographic areas representing all forested biogeographic and climate zones. This represents an 175% increase in records from the prior publication (Anderson-Teixeira *et al* 2018).

Here, we analyze the more extensive *ForC* data (Fig. 1) to provide a robust overview of stand-level carbon cycling of the world's major forest biomes and how it varies with stand age. Our primary goal is to provide a data-driven summary of our current state of knowledge on broad trends in forest C cycling. Specifically, we address three broad questions:

1. How thoroughly can we represent C budgets for each of the world's major forest biomes (*i.e.*, tropical, temperate broadleaf and deciduous, boreal) based on the current *ForC* data?
2. How do C cycling vary across the world's major forest biomes?
3. How does C cycling vary with stand age (in interaction with biome)?

While components of these questions have been previously addressed (Luyssaert *et al* 2007, Anderson-Teixeira *et al* 2016, Cook-Patton *et al* 2020, Banbury Morgan *et al* n.d.), our analysis represents by far the most comprehensive analysis of C cycling in global forests, and will serve as a foundation for improved understanding of global forest C cycling and highlight where key sources of uncertainty still reside.

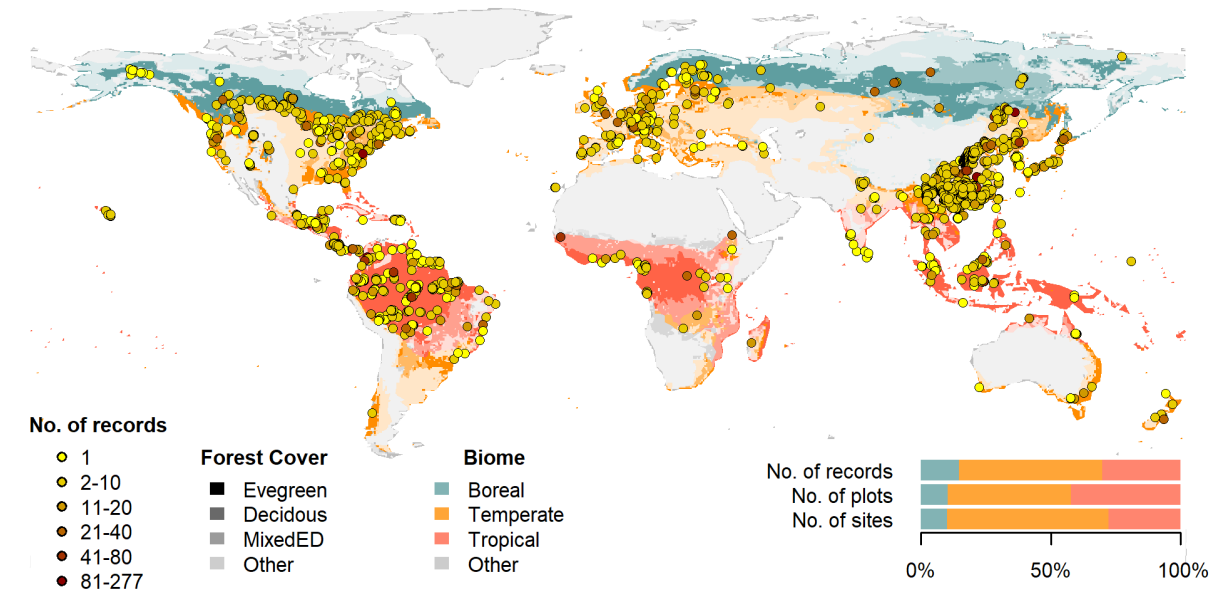


Figure 1 | Map of sites included in this analysis. Symbols are colored according to the number of records at each site. Underlying map shows coverage of evergreen, deciduous, and mixed forests (from SYNMAP; Jung et al. 2006) and biomes. Distribution of sites, plots, and records among biomes is shown in the inset.

118 Methods/ Design

119 This review synthesizes data from the *ForC* database (Fig. 1; <https://github.com/forc-db/ForC>;

120 Anderson-Teixeira *et al* 2016, pp @anderson-teixeira_forc_2018). *ForC* amalgamates numerous

121 intermediary data sets (*e.g.*, Luyssaert *et al* 2007, Bond-Lamberty and Thomson 2010, Cook-Patton *et al*

122 2020) and original studies. Original publications were referenced to check values and obtain information not

123 contained in intermediary data sets, although this process has not been completed for all records. The

124 database was developed with goals of understanding how C cycling in forests varies across broad geographic

125 scales and as a function of stand age. As such, there has been a focus on incorporating data from regrowth

126 forests (*e.g.*, Anderson *et al* 2006, Martin *et al* 2013, Bonner *et al* 2013) and obtaining stand age data when

127 possible (83% of records in v.2.0; Anderson-Teixeira *et al* 2018). Particular attention was given to developing

128 the database for tropical forests (Anderson-Teixeira *et al* 2016), which represented roughly one-third of

129 records in *ForC* v.2.0* (Anderson-Teixeira *et al* 2018). Since publication of *ForC* v.2.0, we added the

130 following data to *ForC*: the Global Database of Soil Respiration Database (*SRDB* v.##, 9488 records;

131 Bond-Lamberty and Thomson 2010), the Global Reforestation Opportunity Assessment database (*GROA*

132 v1.0, 18143 records; Cook-Patton *et al* 2020, Anderson-Teixeira *et al* 2020). We've also added data from

133 individual publications (detailed list at [https://github.com/forc-](https://github.com/forc-db/ForC/blob/master/database_management_records/ForC_data_additions_log.csv)

134 db/ForC/blob/master/database_management_records/ForC_data_additions_log.csv), with a particular

135 focus on productivity (Banbury Morgan *et al* n.d., *e.g.*, Taylor *et al* 2017), dead wood, and ForestGEO sites

136 (*e.g.*, Lutz *et al* 2018, p @johnson_climate_2018). We note that there remains a significant amount of

137 relevant data that is not yet included in *ForC*, particularly biomass data from national forest inventories

138 (e.g.,; **REFS**). The database version used for this analysis has been tagged as a new release on Github (**XX**)
139 and assigned a DOI through Zenodo (DOI: TBD).

140 To facilitate analyses, we created a simplified version of ForC, *ForC-simplified*
141 (https://github.com/forc-db/ForC/blob/master/ForC_simplified), which we analyzed here. In generating
142 *ForC-simplified*, all measurements originally expressed in units of dry organic matter (*OM*) were converted
143 to units of C using the IPCC default of $C = 0.47 * OM$ (IPCC 2006). Duplicate or otherwise conflicting
144 records were reconciled as described in APPENDIX S1, resulting in a total of 32499 records (67.9% size of
145 total database). Records were filtered to remove plots that had undergone significant anthropogenic
146 management or major disturbance since the most recent stand initiation event. Specifically, we removed all
147 plots flagged as managed in ForC-simplified (18.9%). This included plots with any record of managements
148 manipulating CO₂, temperature, hydrology, nutrients, or biota, as well as any plots whose site or plot name
149 contained the terms “plantation”, “planted”, “managed”, “irrigated”, or “fertilized”. Plots flagged as
150 disturbed in ForC-simplified (5.7%) included stands that had undergone any notable anthropogenic thinning
151 or partial harvest. We retained sites that were grazed or had undergone low severity natural disturbances
152 (<10% mortality) including droughts, major storms, fires, and floods. We removed all plots for which no
153 stand history information had been retrieved (7.3%). In total, this resulted in 23199 records (48.5% of the
154 records in the database) being eligible for inclusion in the analysis.

155 We selected 23 annual flux and 11 C stock variables for inclusion in the analysis. These different flux and
156 stock variables (Table 1) represent different pools (e.g., aboveground biomass, dead wood, ecosystem total)
157 and levels of combination (e.g., total aboveground net primary productivity (*ANPP*) versus the ANPP of
158 individual elements such as foliage, roots, and branches. Note that two flux variables, aboveground
159 heterotrophic (R_{het-ag}) and total (R_{het}) respiration, were included for conceptual completeness but had no
160 records in *ForC* (Table 1). Records for these variables represented 68.6% of the total records eligible for
161 inclusion. For this analysis, we combined some of ForC’s specific variables (e.g., multiple variables for net
162 primary productivity, such as measurements including or excluding fruit and flower production and herbivory)
163 into more broadly defined variables. Specifically, net ecosystem exchange (measured by eddy-covariance;
164 **FLUXNET REF**) and biometric estimates of *NEP* were combined into the single variable *NEP* (Table 1).
165 Furthermore, for *NPP*, *ANPP*, and *ANPP_{litterfall}*, *ForC* variables specifying inclusion of different
166 components were combined. Throughout ForC, for all measurements drawing from tree census data (e.g.,
167 biomass, productivity), the minimum diameter breast height (DBH) threshold for tree census was $\leq 10\text{cm}$.
168 All records were measured directly or derived from field measurements (as opposed to modeled).

169 For this analysis, we grouped forests into four broad biome types based on climate zones and dominant
170 vegetation type (tropical broadleaf, temperate broadleaf, temperate needleleaf, and boreal needleleaf) and
171 two age classifications (young and mature). Climate zones (Fig. 1) were defined based on site geographic
172 coordinates according to Köppen-Geiger zones (Rubel and Kottek 2010). We defined the tropical biome as
173 including all equatorial (A) zones, temperate biomes as including all warm temperate (C) zones and warmer
174 snow climates (Dsa, Dsb, Dwa, Dwb, Dfa, and Dfb), and the boreal biome as including the colder snow
175 climates (Dsc, Dsd, Dwc, Dwd, Dfc, and Dfd). Any forests in dry (B) and polar (E) Köppen-Geiger zones
176 were excluded from the analysis. We defined leaf type (broadleaf / needleleaf) was based on descriptions in
177 original publications (prioritized) or values extracted from a global map based on satellite observations
178 (SYNMAP; ???). For young tropical forests imported from *GROA* but not yet classified by leaf type, we
179 assumed that all were broadleaf, consistent with the rarity of naturally regenerating needleleaf forests in the

Table 1. Carbon cycle variables included in this analysis, their sample sizes, and summary of biome differences and age trends.

Variable	Description	N records			biome differences*	age trend†
		records	plots	geographic areas		
Annual fluxes						
<i>NEP</i>	net ecosystem production or net ecosystem exchange (+ indicates C sink)	329	146	88	n.s.	+; xB
<i>GPP</i>	gross primary production ($NPP + R_{auto}$ or $R_{eco} - NEE$)	303	115	84	$TrB > TeB \geq TeN \geq BoN$	+; xB
<i>NPP</i>	net primary production ($ANPP + BNPP$)	214	112	74	$TrB > TeB \geq TeN > BoN$	n.s.
<i>ANPP</i>	aboveground <i>NPP</i>	343	236	131	$TrB > TeB \geq TeN > BoN$	+; xB
<i>ANPP_{woody}</i>	woody production ($ANPP_{stem} + ANPP_{branch}$)	64	53	37	n.s.	+
<i>ANPP_{stem}</i>	woody stem production	217	190	117	$TrB > TeN \geq TeB \geq BoN$	n.s.
<i>ANPP_{branch}</i>	branch turnover	69	59	42	$TrB > TeB \geq TeN$	n.s.
<i>ANPP_{foliage}</i>	foliage production, typically estimated as annual leaf litterfall	162	132	88	$TrB > TeB \geq TeN > BoN$	+
<i>ANPP_{litterfall}</i>	litterfall, including leaves, reproductive structures, twigs, and sometimes branches	82	70	55	n.s.	+
<i>ANPP_{repro}</i>	production of reproductive structures (flowers, fruits, seeds)	51	44	34	-	-
<i>ANPP_{folivory}</i>	foliar biomass consumed by folivores	20	12	11	-	-
<i>M_{woody}</i>	woody mortality—i.e., B_{ag} of trees that die	18	18	18	-	-
<i>BNPP</i>	belowground NPP ($BNPP_{coarse} + BNPP_{fine}$)	148	116	79	$TrB > TeN \geq TeB \geq BoN$	+
<i>BNPP_{coarse}</i>	coarse root production	77	56	36	$TeN \geq TrB$	n.s.
<i>BNPP_{fine}</i>	fine root production	123	99	66	n.s.	+
<i>R_{eco}</i>	ecosystem respiration ($R_{auto} + R_{het}$)	213	98	70	$TrB > TeB \geq TeN$	+
<i>R_{auto}</i>	autotrophic respiration ($(R_{auto-ag} + R_{root})$)	24	23	15	-	-
<i>R_{auto-ag}</i>	aboveground autotrophic respiration (i.e., leaves and stems)	2	2	1	-	-
<i>R_{root}</i>	root respiration	181	139	95	$TrB \geq TeB$	+
<i>R_{soil}</i>	soil respiration ($R_{het-soil} + R_{root}$)	627	411	229	$TrB > TeB > TeN \geq BoN$	n.s.
<i>R_{het-soil}</i>	soil heterotrophic respiration	197	156	100	$TrB > TeB \geq TeN$	n.s.
<i>R_{het-ag}</i>	aboveground heterotrophic respiration	0	0	0	-	-
<i>R_{het}</i>	heterotrophic respiration ($(R_{het-ag} + R_{het-soil})$)	0	0	0	-	-
Stocks						
<i>B_{tot}</i>	total live biomass ($B_{ag} + B_{root}$)	188	157	87	$TrB \geq TeB > BoN$	+; xB
<i>B_{ag}</i>	aboveground live biomass ($B_{ag-wood} + B_{foliage}$)	4666	4272	625	$TrB \geq TeN \geq TeB > BoN$	+; xB
<i>B_{ag-wood}</i>	woody component of aboveground biomass	115	102	64	$TeN > TrB \geq BoN$	+; xB
<i>B_{foliage}</i>	foliage biomass	134	115	72	$TeN > TrB \geq BoN \geq TeB$	+; xB
<i>B_{root}</i>	total root biomass ($B_{root-coarse} + B_{root-fine}$)	2330	2299	361	n.s.	+; xB
<i>B_{root-coarse}</i>	coarse root biomass	134	120	73	$TeN > TeB \geq BoN$	+; xB
<i>B_{root-fine}</i>	fine root biomass	226	180	109	n.s.	+; xB
<i>DW_{tot}</i>	deadwood ($DW_{standing} + DW_{down}$)	79	73	42	-	+; xB
<i>DW_{standing}</i>	standing dead wood	36	35	22	-	-
<i>DW_{down}</i>	fallen dead wood, including coarse and sometimes fine woody debris	278	265	37	-	+; xB
<i>OL</i>	organic layer / litter/ forest floor	474	413	115	n.s.	+; xB

* Tr: Tropical, TeB: Temperate Broadleaf, TeN: Temperate Needleleaf, B: Boreal, n.s.: no significant differences

† + or -: significant positive or negative trend, xB: significant age x biome interaction, n.s.: no significant age trend

180 tropics (**REF**). We also classified forests as “young” (< 100 years) or “mature” (≥ 100 years or classified as
181 “mature”, “old growth”, “intact”, or “undisturbed” in original publication). Assigning stands to these
182 groupings required the exclusion of records for which *ForC* lacked geographic coordinates (0.4% of sites in
183 full database) or records of stand age (4.8% of records in full database). We also excluded records of stand
184 age = 0 year (0.8% of records in full database). In total, our analysis retained 76.2 of the focal variable
185 records for forests of known age. Numbers of records by biome and age class are given in Table S1.

186 Data were summarized to produce schematics of C cycling across the eight biome by age group combinations
187 identified above. To obtain the values reported in the C cycle schematics, we first averaged any repeated
188 measurements within a plot. Values were then averaged across geographically distinct areas, defined as plots
189 clustered within 25 km of one another (*sensu* Anderson-Teixeira *et al* 2018), weighting by area sampled if
190 available for all records. This step was taken to avoid pseudo-replication and to combine any records from
191 sites with more than one name in ForC.

192 We tested whether the C budgets described above “closed”—*i.e.*, whether they were internally consistent.
193 Specifically, we first defined relationships among variables: for example, $NEP = GPP - R_{eco}$,
194 $BNPP = BNPP_{coarse} + BNPP_{fine}$, $DW_{tot} = DW_{standing} + DW_{down}$. (**issue #44—but just delete**
195 **this chunk if not resolved before submission**) Henceforth, we refer to the variables on the left side of
196 the equation as “aggregate” fluxes or stocks, and those that are summed as “component” fluxes or stocks,
197 noting that the same variable can take both aggregate and component positions in different relationships.
198 We considered the C budget for a given relationship “closed” when component variables summed to within
199 one standard deviation of the aggregate variable.

200 To test for differences across mature forest biomes, we also examined how stand age impacted fluxes and
201 stocks, employing a mixed effects model [‘lmer’ function in ‘lme4’ R package version **x.xx**; **REF**] with biome
202 as fixed effect and plot nested within geographic.area as random effects on the intercept. When Biome had a
203 significant effect, we looked at a Tukey’s pairwise comparison to see which biomes were significantly different
204 from one another. This analysis was run for variables with records for at least seven distinct geographic areas
205 in more than one biome, excluding any biomes that failed this criteria (Table 1).

206 To test for age trends in young (<100yrs) forests, we employed a mixed effects model with biome and
207 $\log_{10}[\text{stand.age}]$ as fixed effects and plot nested within geographic.area as a random effect on the intercept.
208 This analysis was run for variables with records for at least three distinct geographic areas in more than one
209 biome, excluding any biomes that failed this criteria (Table 1). When the effect of stand age was significant
210 at $p \leq 0.05$ and when each biome had records for stands of at least 10 different ages, a biome \times stand.age
211 interaction was included in the model.

212 To facilitate the accessibility of our results and data, and to allow for rapid updates as additional data
213 become available, we have automated all database manipulation, analyses, and figure production in R
214 (**version, citation**).

215 Review Results/ Synthesis

216 Data Coverage

217 Of the 47837 records in *ForC* v3.0, 12124 met our strict criteria for inclusion in this study (Fig. 1). These
218 records were distributed across 5262 plots in 869 distinct geographic areas. Of the 23 flux and 11 stock

variables mapped in these diagrams, *ForC* contained sufficient mature forest data for inclusion in our statistical analyses (*i.e.*, records from ≥ 7 distinct geographic areas, and number of distinct plots < number of observations) for 20 fluxes and 9 stocks in tropical broadleaf forests, 15 fluxes and 8 stocks in temperate broadleaf forests, 14 fluxes and 7 stocks in temperate conifer forests, and 8 fluxes and 7 stocks in boreal forests. For regrowth forests (<100 yrs), *ForC* contained sufficient data for inclusion in our statistical analyses (*i.e.*, records from ≥ 3 distinct geographic areas, and number of distinct plots < number of observations) for 11 fluxes and 10 stocks in tropical broadleaf forests, 16 fluxes and 10 stocks in temperate broadleaf forests, 16 fluxes and 10 stocks in temperate conifer forests, and 14 fluxes and 9 stocks in boreal forests.

228 C cycling in mature forests

Average C cycles for mature tropical broadleaf, temperate broadleaf, temperate conifer, and boreal forests \geq 100 years old and with no known major natural or anthropogenic disturbance are presented in Figures 2-5 (and available in tabular format in the *ForC* release accompanying this publication:

`ForC/numbers_and_facts/ForC_variable_averages_per_Biome.csv`.

For variables with records from ≥ 7 distinct geographic areas, these ensemble C budgets were generally consistent. *That is, component variables summed to within one standard deviation of their respective aggregate variables in all but two instances, both in temperate conifer forests (Fig. 5). (check all this with final results:*

https://github.com/forc-db/ForC/blob/master/numbers_and_facts/C_cycle_closure.csv,

and be sure to write out variable names at first occurrence, and provide a bit more detail)

For the temperate conifer biome, the average composite measure of aboveground biomass (B_{ag}) was less than the combined average value of woody biomass ($B_{ag-wood}$) and foliage biomass ($B_{foliage}$), partly due to the very high estimates of $B_{ag-wood}$. Within this biome, $B_{ag} < B_{ag-wood} + B_{foliage}$ and

$B_{root} < B_{root-coarse} + B_{root-fine}$ because $B_{ag-wood}$ and $B_{root-coarse}$ were very high, with strongly disproportionate numbers of records from the high-biomass forests of the US Pacific Northwest (Figs. S18, S21).

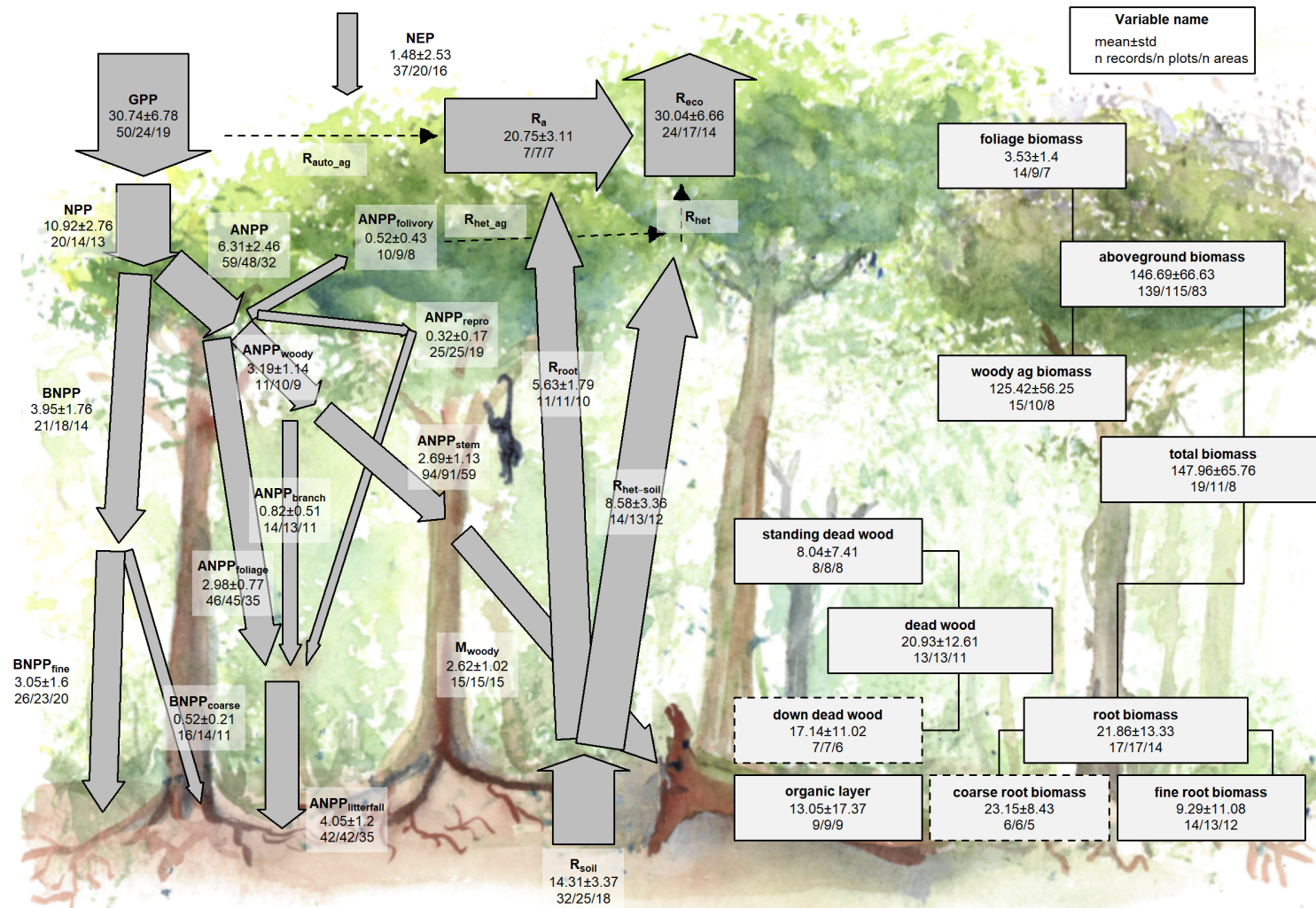


Figure 2 | C cycle diagram for mature tropical broadleaf forests. Arrows indicate fluxes ($Mg\ C\ ha^{-1}\ yr^{-1}$); boxes indicate stocks ($Mg\ C\ ha^{-1}$), with variables as defined in Table 1. Presented are mean \pm std, where geographically distinct areas are treated as the unit of replication. Dashed shape outlines indicate variables with records from <7 distinct geographic areas, and dashed arrows indicate fluxes with no data. To illustrate the magnitude of different fluxes, arrow size is proportional to the square root of corresponding flux. Asterisk after variable name indicates lack of C cycle closure.

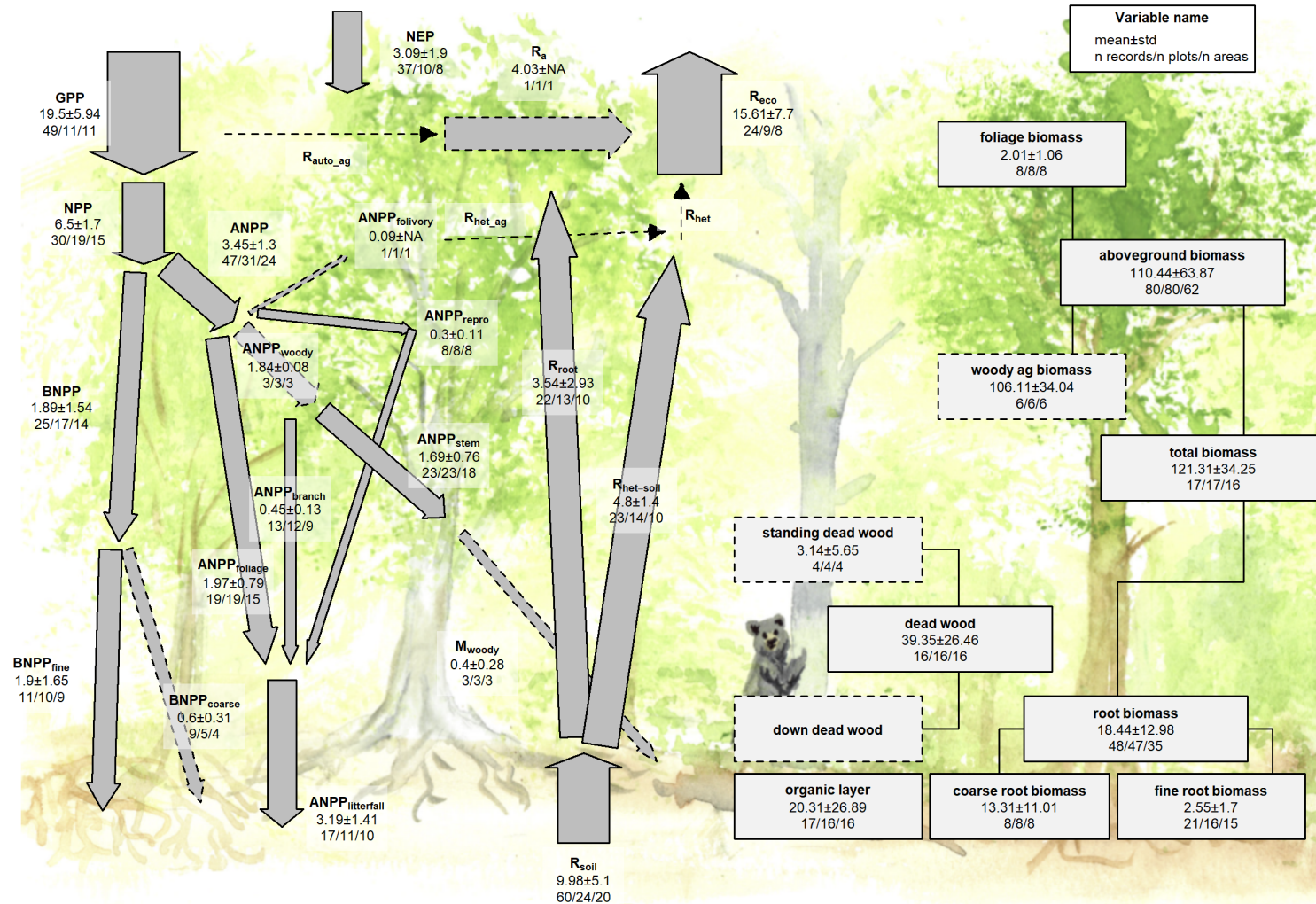


Figure 3 | C cycle diagram for mature temperate broadleaf forests. Arrows indicate fluxes ($\text{Mg C ha}^{-1} \text{ yr}^{-1}$); boxes indicate stocks (Mg C ha^{-1}), with variables as defined in Table 1. Presented are mean \pm std, where geographically distinct areas are treated as the unit of replication. Dashed shape outlines indicate variables with records from <7 distinct geographic areas, and dashed arrows indicate fluxes with no data. To illustrate the magnitude of different fluxes, arrow size is proportional to the square root of corresponding flux. Asterisk after variable name indicates lack of C cycle closure.

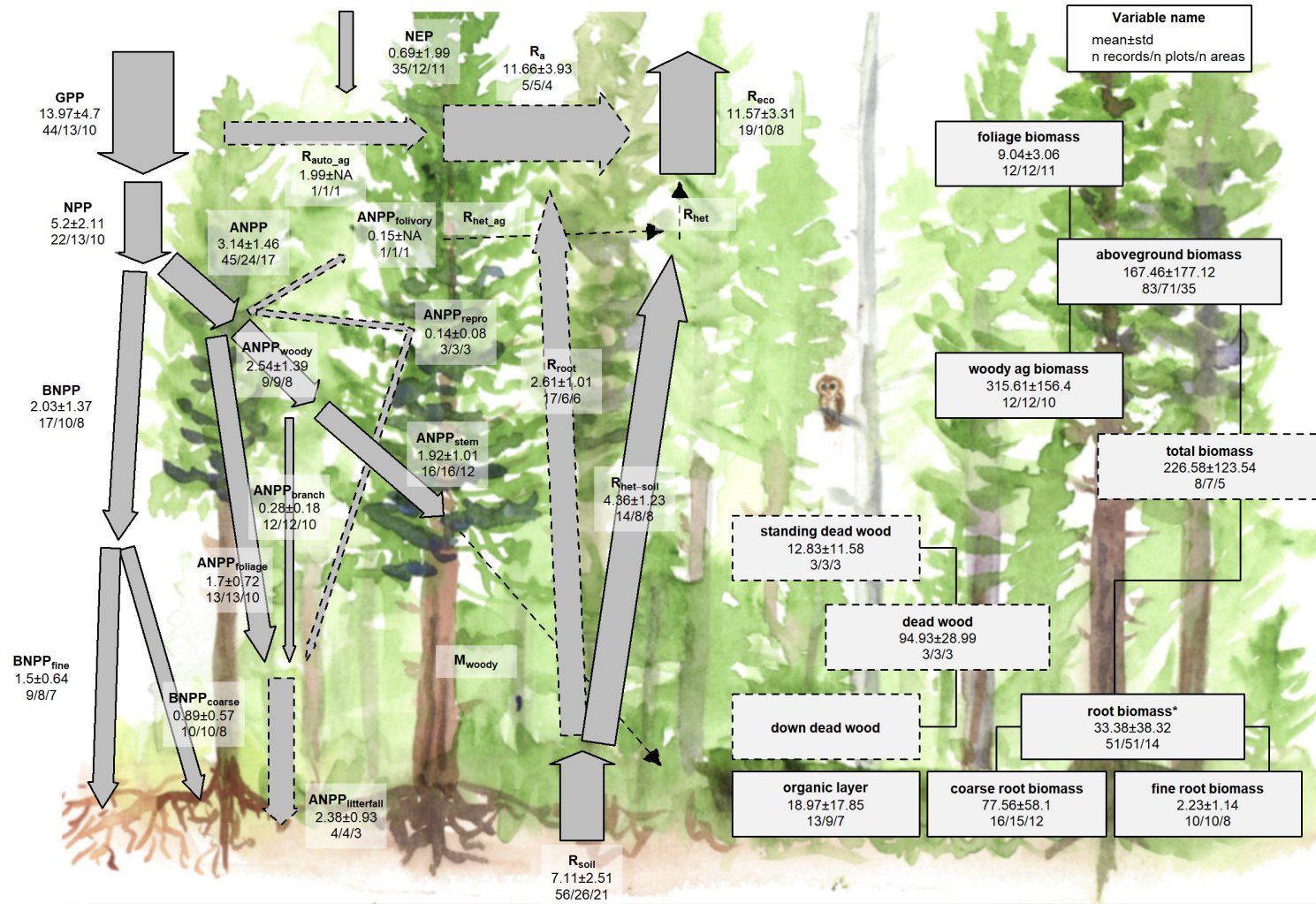


Figure 4 | C cycle diagram for mature temperate conifer forests. Arrows indicate fluxes ($\text{Mg C ha}^{-1} \text{ yr}^{-1}$); boxes indicate stocks (Mg C ha^{-1}), with variables as defined in Table 1. Presented are mean \pm std, where geographically distinct areas are treated as the unit of replication. Dashed shape outlines indicate variables with records from <7 distinct geographic areas, and dashed arrows indicate fluxes with no data. To illustrate the magnitude of different fluxes, arrow size is proportional to the square root of corresponding flux. Asterisk after variable name indicates lack of C cycle closure.

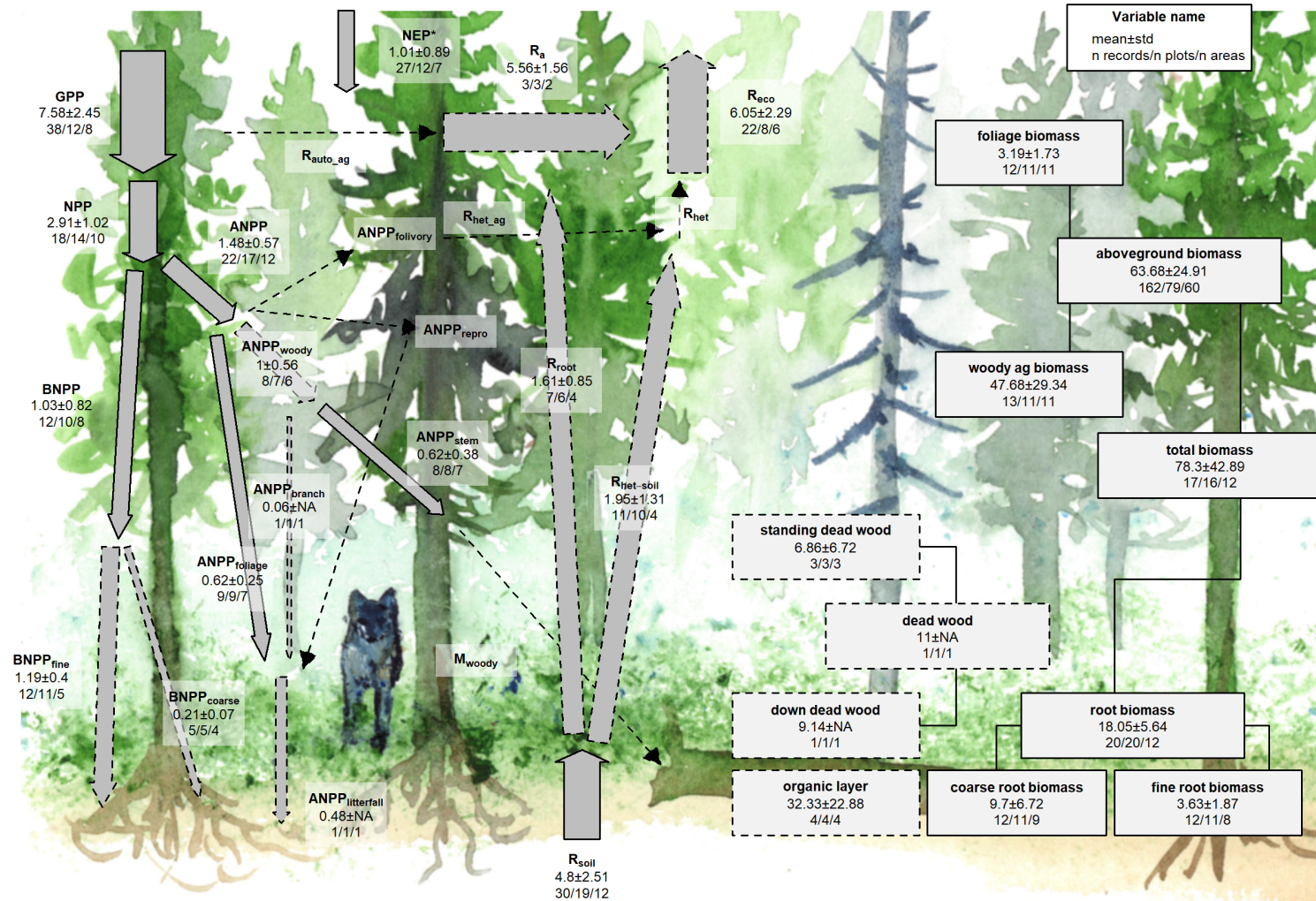


Figure 5 | C cycle diagram for mature boreal conifer forests. Arrows indicate fluxes ($\text{Mg C ha}^{-1} \text{ yr}^{-1}$); boxes indicate stocks (Mg C ha^{-1}), with variables as defined in Table 1. Presented are mean \pm std, where geographically distinct areas are treated as the unit of replication. Dashed shape outlines indicate variables with records from <7 distinct geographic areas, and dashed arrows indicate fluxes with no data. To illustrate the magnitude of different fluxes, arrow size is proportional to the square root of corresponding flux. Asterisk after variable name indicates lack of C cycle closure.

245 **check this with final data (based on Table 1):** There were sufficient data to assess mature forest
246 biome differences for **20** flux variables, and significant differences among biomes were detected for **14**
247 variables (Table 1). In all cases—including C fluxes into, within, and out of the ecosystem—C fluxes were
248 highest in tropical forests, intermediate in temperate (broadleaf or conifer) forests, and lowest in boreal
249 forests (Table 1, Figs. 6, S1-S15). Differences between tropical and boreal forests were always significant,
250 with temperate forests intermediate and significantly different from one or both. Fluxes tended to be
251 numerically greater in temperate broadleaf than conifer forests, but the difference was never statistically
252 significant. This pattern held for the following variables: **** GPP , NPP , $ANPP$, $ANPP_{woody}$,**
253 **$ANPP_{stem}$, $ANPP_{branch}$, $ANPP_{foliage}$, $ANPP_{litterfall}$, M_{woody} , $BNPP$, R_{eco} , R_{soil} , and $R_{het-soil}$ **.** For
254 variables without significant differences among biomes, the same general trends applied.

255 The most notable exception to this pattern was NEP , with no significant differences across biomes but with
256 the largest average in temperate broadleaf forests, followed by temperate conifer, boreal, and tropical forests
257 (Figs. 5,S1). Another exception was for $BNPP_{root-coarse}$, where all records came from high-biomass forests
258 in the US Pacific Northwest, resulting in high values for the temperate conifer biome and no significant
259 differences across biomes (Fig. S10).

260 Thus, C cycling rates generally decreased from tropical to temperate to boreal forests, with the important
261 exception in the overall C balance (NEP).

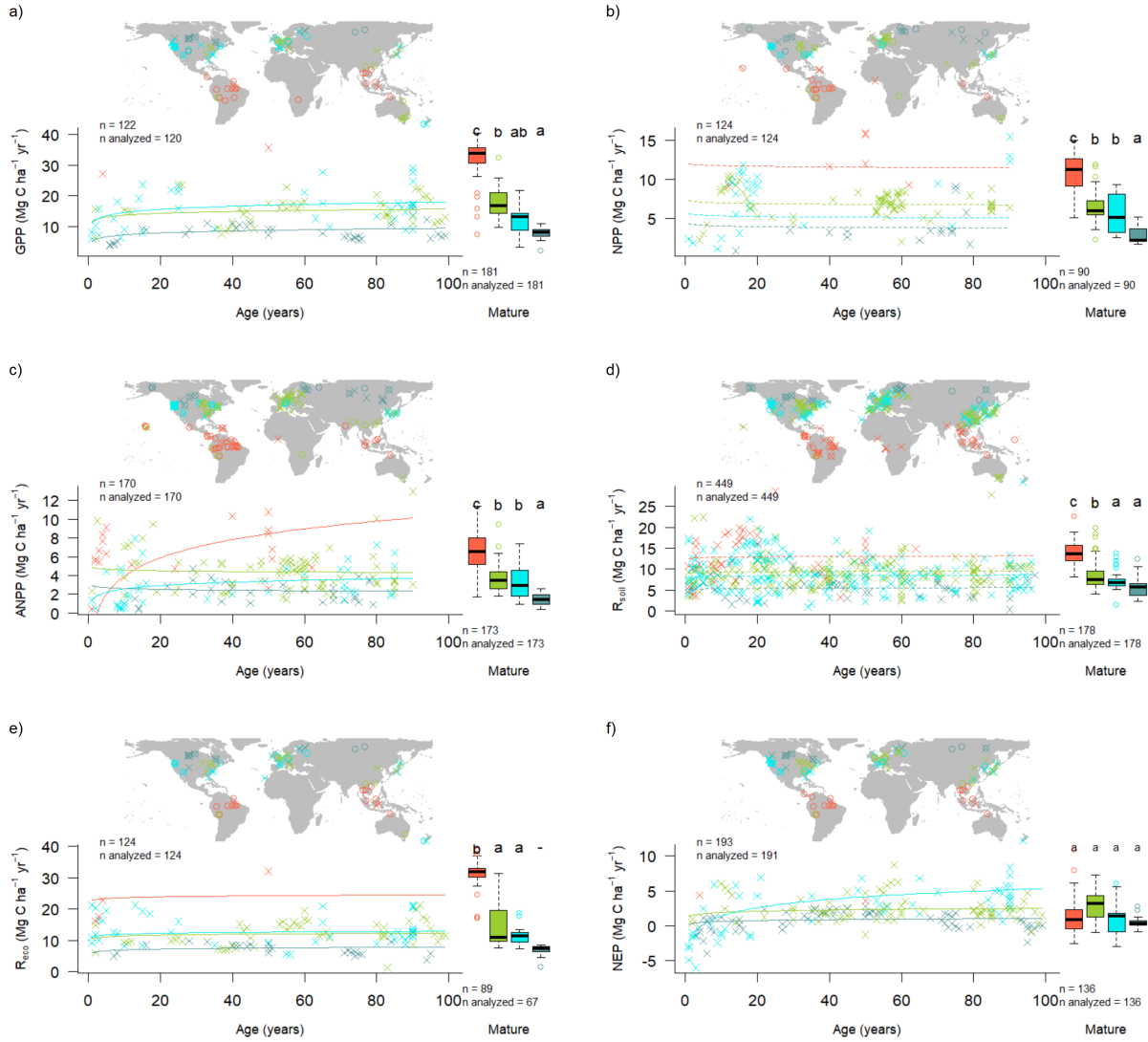


Figure 6 | Age trends and biome differences in some of the major C fluxes: (a) GPP , (b) NPP , (c) $ANPP$, (d) R_{soil} , (e) R_{eco} , and (f) NEP . Map shows data sources (x and o indicate young and mature stands, respectively). In each panel, the left scatterplot shows age trends in forests up to 100 years old, as characterized by a linear mixed effects model with fixed effects of age and biome. The fitted line indicates the effect of age on flux (solid lines: significant at $p < 0.05$, dashed lines: non-significant), and non-parallel lines indicate a significant age \times biome interaction. The boxplot illustrates distribution across mature forests, with different letters indicating significant differences between biomes. Data from biomes that did not meet the sample size criteria (see Methods) are plotted, but lack regression lines (young forests) or test of differences across biomes (mature forests). Individual figures for each flux with sufficient data are given in the Supplement (Figs. S1-S15).

262 **check this with final data (based on Table 1):** There were sufficient data to assess mature forest
 263 biome differences for **9** stock variables, and significant differences among biomes were detected for **6** variables
 264 (B_{tot} , B_{ag} , $B_{ag-wood}$, $B_{foliage}$, $B_{root-coarse}$, DW_{tot} ; Table 1). C stocks had less consistent patterns across
 265 biomes (Figs. 7, S16-S26). In **four of the six** cases (B_{tot} , $B_{ag-wood}$, $B_{root-coarse}$, DW_{tot}), temperate
 266 conifer forests had significantly higher stocks than the other biomes, and boreal forests in the lowest, with
 267 tropical and temperate broadleaf forests in between. For B_{ag} , which had by far the highest sample size,
 268 tropical forests exceeded temperate conifer forests (but not significantly). For $B_{foliage}$, temperate broadleaf
 269 forests were lowest (again, not significantly). The high values for the temperate conifer biome were driven by

270 the very high-biomass forests of the US Pacific Northwest, which are disproportionately represented in the
 271 current version of ForC. Thus, biome differences should be interpreted more as driven more by geographic
 272 distribution of sampling than by true differences.

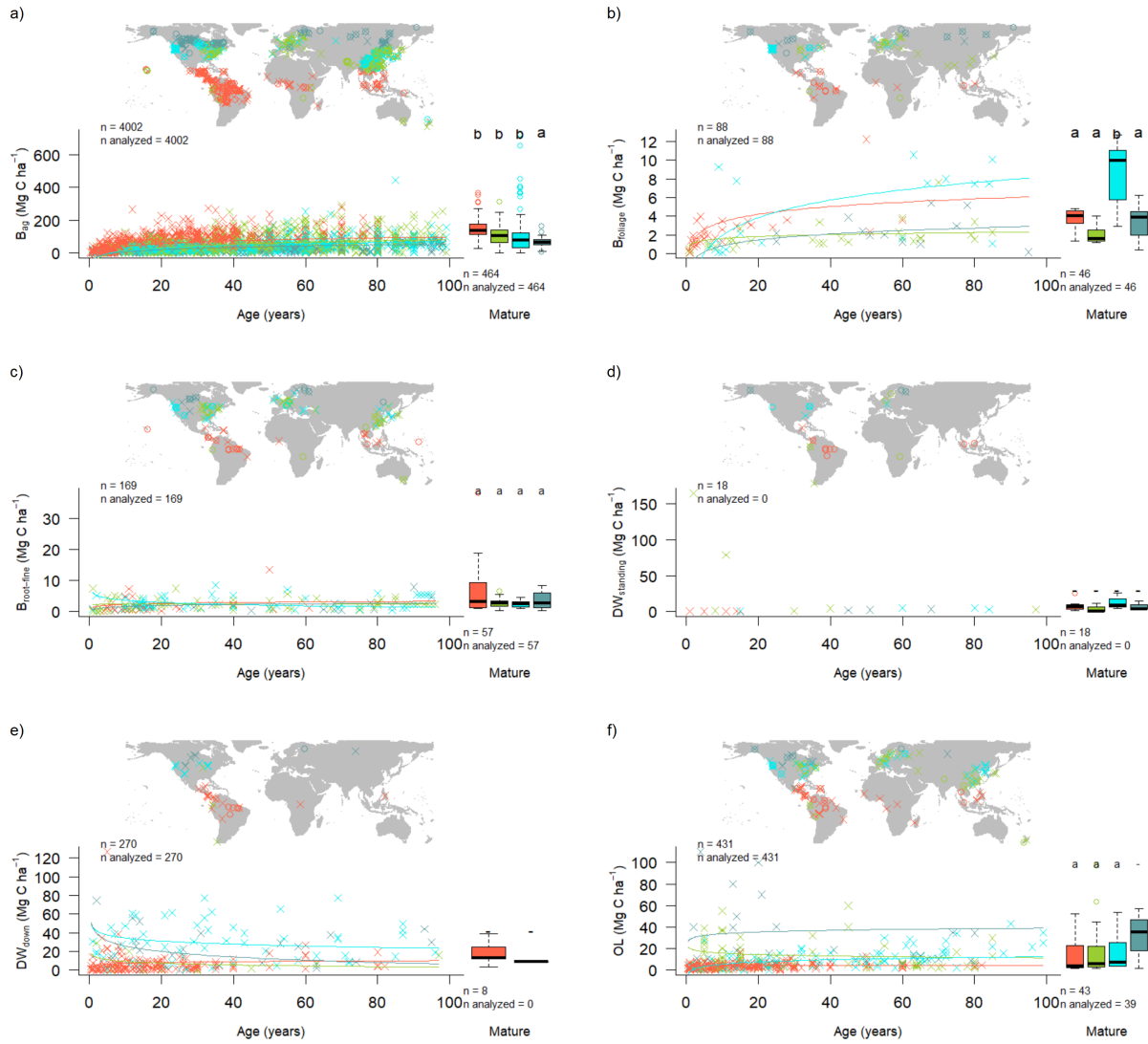


Figure 7 | Age trends and biome differences in some of the major forest C stocks: (a) aboveground biomass, (b) foliage, (c) fine roots, (d) dead wood. Map shows data sources (x and o indicate young and mature stands, respectively). In each panel, the left scatterplot shows age trends in forests up to 100 years old, as characterized by a linear mixed effects model with fixed effects of age and biome. The fitted line indicates the effect of age on flux (solid lines: significant at $p < 0.05$, dashed lines: non-significant), and non-parallel lines indicate a significant age x biome interaction. The boxplot illustrates distribution across mature forests, with different letters indicating significant differences between biomes. Data from biomes that did not meet the sample size criteria (see Methods) are plotted, but lack regression lines (young forests) or test of differences across biomes (mature forests). Individual figures for each stock with sufficient data are given in the Supplement (Figs. S16-S26).

273 C cycling in young forests

274 Average C cycles for forests < 100 years old are presented in Figures 8-11.
 275 Both C stocks and fluxes commonly increased significantly with stand age (Tables 1, S2, Figs. 6-11, S1-S26;
 276 detailed below).

277 *ForC* contained 14 flux variables with sufficient data for cross-biome analyses of age trends in regrowth
278 forests (see Methods) (Fig. 6-7 and **S#- SI figures including plots for all variables**). Of these, 9
279 increased significantly with age: *GPP*, *NPP*, *ANPP*, *ANPP_{foliage}*, *ANPP_{woody}*, *ANPP_{woody-stem}*,
280 *BNPP*, *BNPP_{root-fine}*, *R_{eco}*, and net C sequestration (*NEP*). The remaining five—*ANPP_{woody-branch}*,
281 *BNPP_{root-coarse}*, *R_{soil-het}*, and *R_{soil-het}*—displayed no significant relationship to stand age, although all
282 displayed a positive trend.

283 Differences in C fluxes across biomes typically paralleled those observed for mature forests, with C cycling
284 generally most rapid in the tropics and slowest in boreal forests.

285 The single exception was *ANPP_{stem}*, for which temperate broadleaf forests and temperate conifer forests of
286 age >~30 had slightly higher flux rates than tropical forests (*represented by a single chronosequence*).

287 Notably, the trend of tropical > temperate > boreal held for *NEP* in regrowth forests, in contrast to the
288 lack of biome differences in *NEP* for mature forests (Fig. 6).

289 There were only ## flux variables with sufficient data to test for biome x age interactions: *ANPP*,
290 *ANPP_{woody}*, *ANPP_{stem}*, *ANPP_{litterfall}*, and *BNPP* (Table S2). (**more could be added if age trends
291 become significant after outliers are resolved**) For three of these (*ANPP*, *ANPP_{litterfall}*, *BNPP*),
292 the increase in C flux with age was steepest increase in tropical forests, followed by temperate and then
293 boreal forests (Figs S#). Similarly, *ANPP_{woody}* displayed a steeper increase with age in temperate than
294 boreal forests (no tropical data for this variable). In contrast, for *ANPP_{stem}*, tropical and temperate
295 broadleaf forests had the highest flux rates at young ages, but were surpassed by temperate conifer forests
296 between ages 20 and 50 (Fig. S6).

297 (**this needs to be updated with latest data**) In terms of C stocks, 10 variables had sufficient data to
298 test for age trends. Six of these—*total biomass*, *aboveground biomass*, *aboveground woody biomass*, *foliage
299 biomass*, *root biomass*, and *coarse root biomass*—increased significantly with $\log_{10}[\text{stand.age}]$. The
300 remaining four displayed non-significant positive trends: *fine root biomass*, *total dead wood*, *standing dead
301 wood*, and *organic layer*. (*discuss rates of increase*)

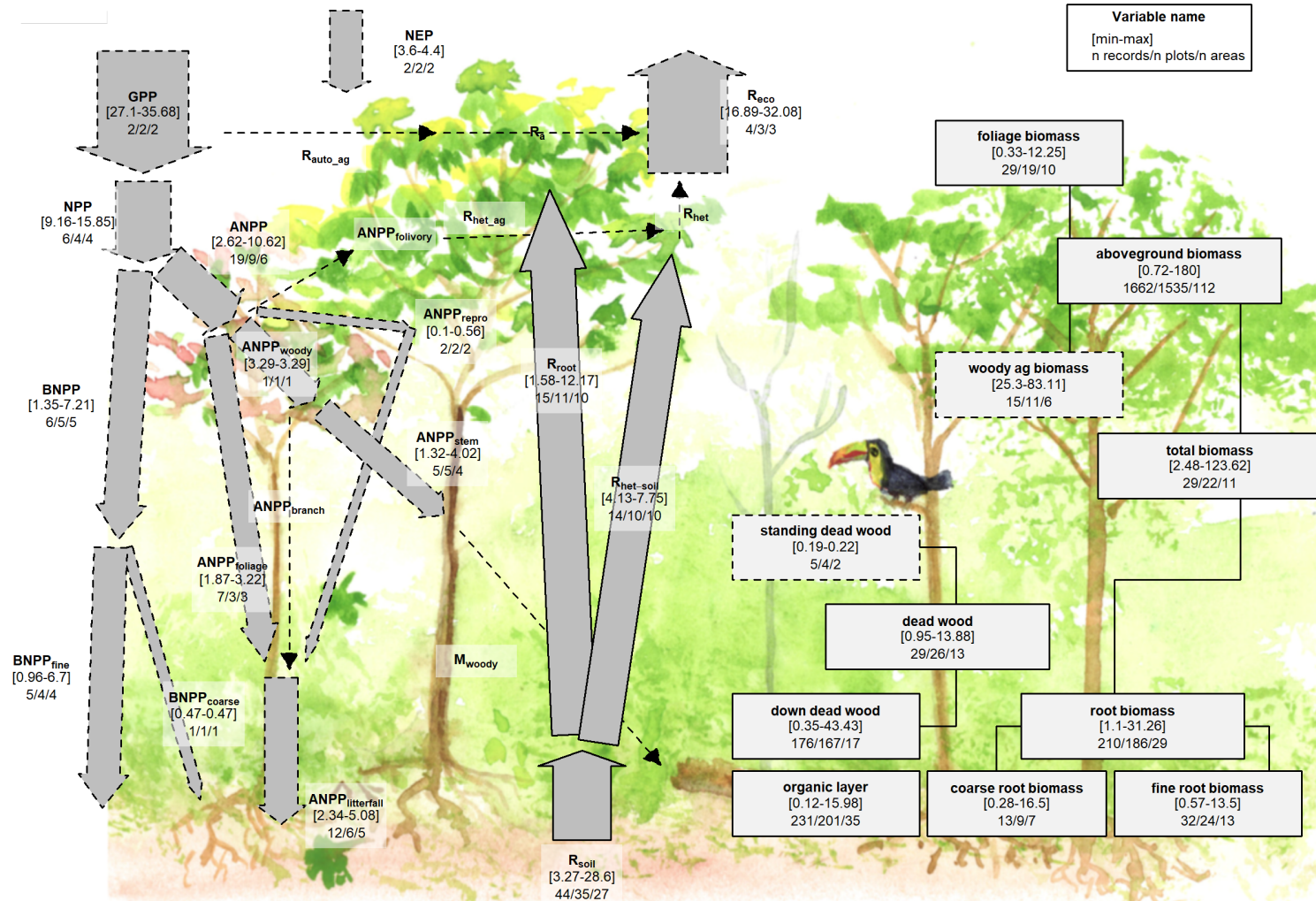


Figure 8 | C cycle diagram for young tropical broadleaf forests. Arrows indicate fluxes ($\text{Mg C ha}^{-1} \text{ yr}^{-1}$); boxes indicate stocks (Mg C ha^{-1}), with variables as defined in Table 1. Presented are observed ranges, where geographically distinct areas are treated as the unit of replication. All units are $\text{Mg C ha}^{-1} \text{ yr}^{-1}$ (fluxes) or Mg C ha^{-1} (stocks). Dashed shape outlines indicate variables with records from <7 distinct geographic areas, and dashed arrows indicate fluxes with no data. To illustrate the magnitude of different fluxes, arrow size is proportional to the square root of corresponding flux.

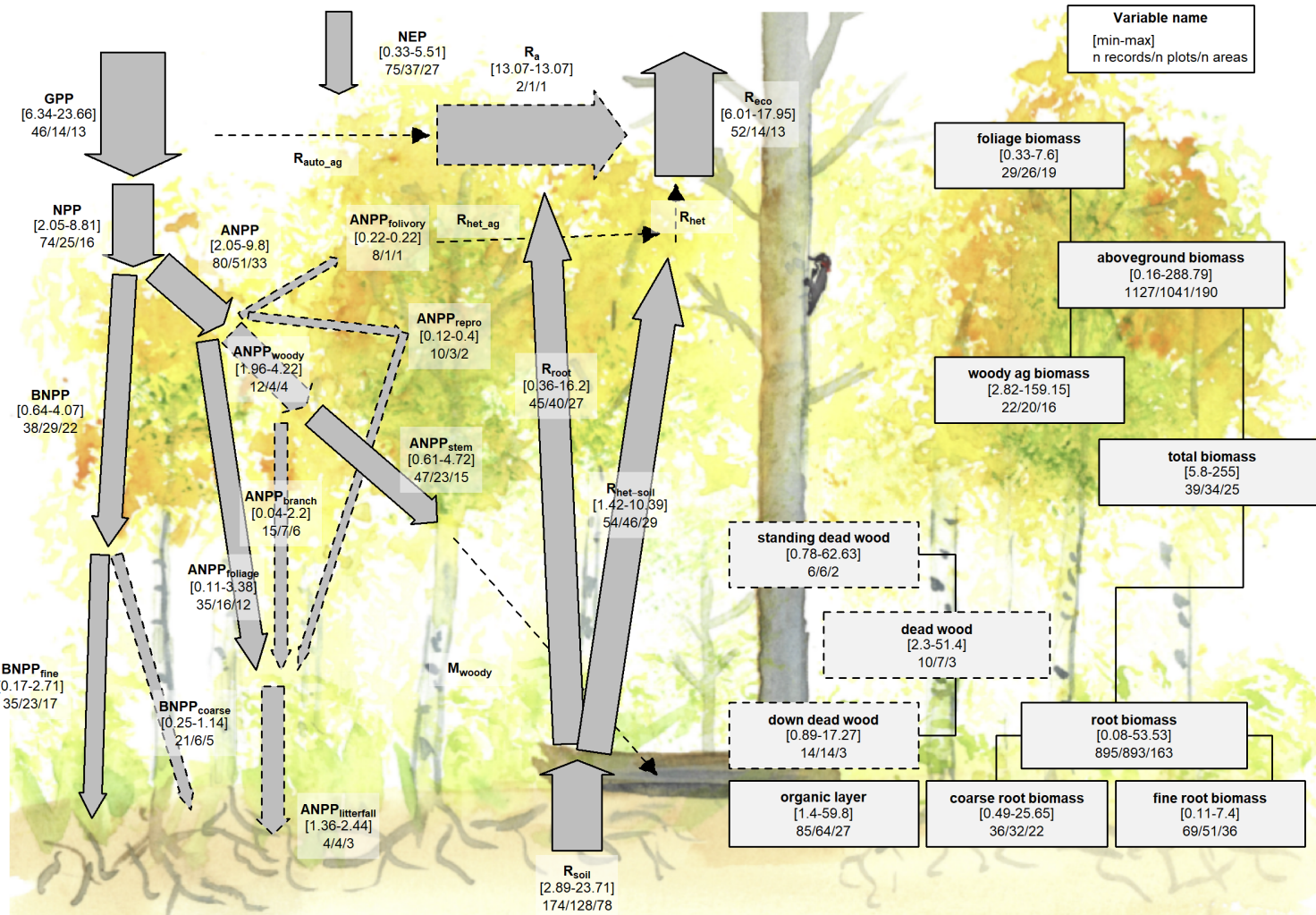


Figure 9 | C cycle diagram for young temperate broadleaf forests. Arrows indicate fluxes ($\text{Mg C ha}^{-1} \text{ yr}^{-1}$); boxes indicate stocks (Mg C ha^{-1}), with variables as defined in Table 1. Presented are observed ranges, where geographically distinct areas are treated as the unit of replication. All units are $\text{Mg C ha}^{-1} \text{ yr}^{-1}$ (fluxes) or Mg C ha^{-1} (stocks). Dashed shape outlines indicate variables with records from <7 distinct geographic areas, and dashed arrows indicate fluxes with no data. To illustrate the magnitude of different fluxes, arrow size is proportional to the square root of corresponding flux.

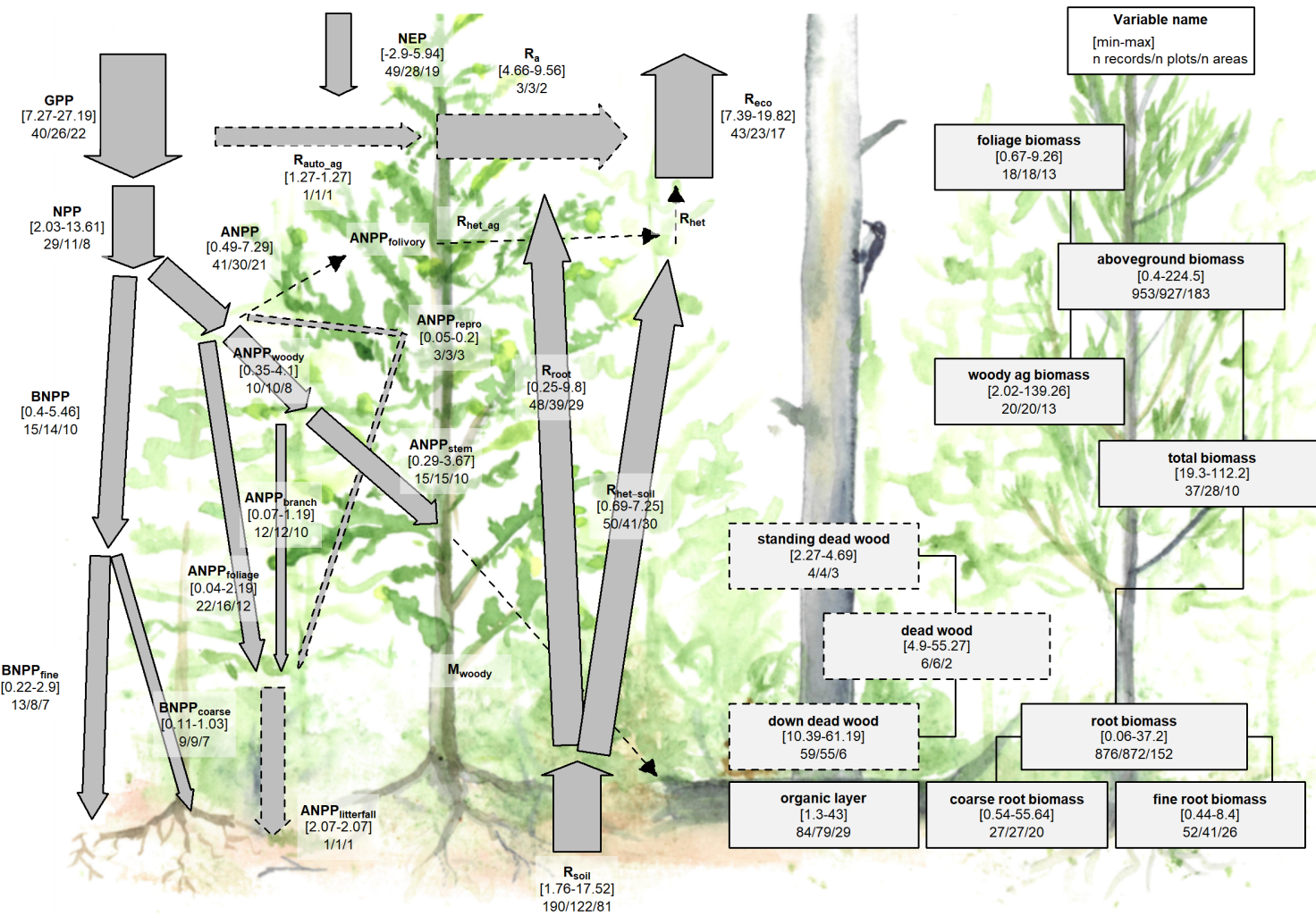


Figure 10 | C cycle diagram for young temperate conifer forests. Arrows indicate fluxes ($\text{Mg C ha}^{-1} \text{ yr}^{-1}$); boxes indicate stocks (Mg C ha^{-1}), with variables as defined in Table 1. Presented are observed ranges, where geographically distinct areas are treated as the unit of replication. All units are $\text{Mg C ha}^{-1} \text{ yr}^{-1}$ (fluxes) or Mg C ha^{-1} (stocks). Dashed shape outlines indicate variables with records from <7 distinct geographic areas, and dashed arrows indicate fluxes with no data. To illustrate the magnitude of different fluxes, arrow size is proportional to the square root of corresponding flux.

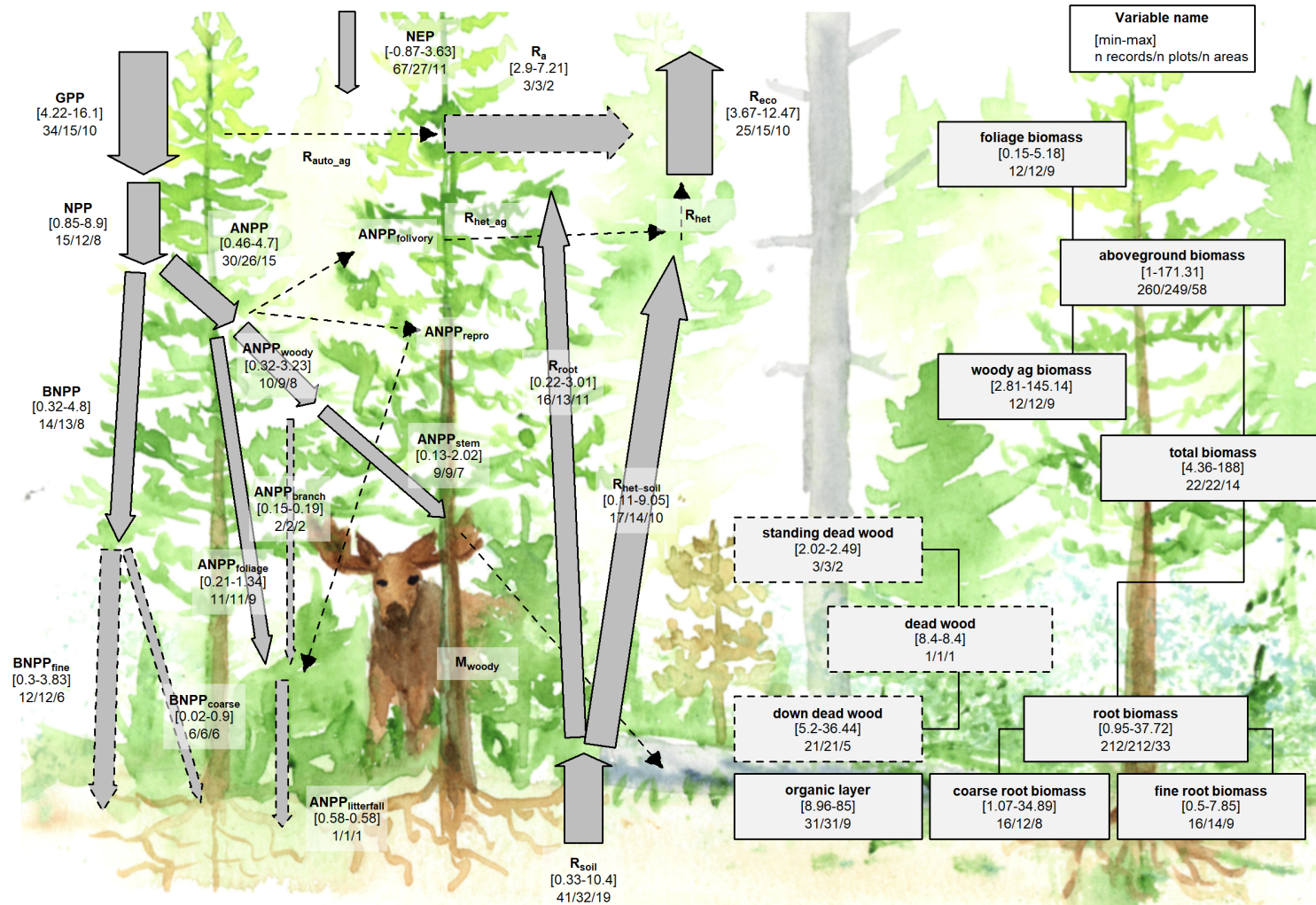


Figure 11 | C cycle diagram for young boreal conifer forests. Arrows indicate fluxes ($Mg\ C\ ha^{-1}\ yr^{-1}$); boxes indicate stocks ($Mg\ C\ ha^{-1}$), with variables as defined in Table 1. Presented are observed ranges, where geographically distinct areas are treated as the unit of replication. All units are $Mg\ C\ ha^{-1}\ yr^{-1}$ (fluxes) or $Mg\ C\ ha^{-1}$ (stocks). Dashed shape outlines indicate variables with records from <7 distinct geographic areas, and dashed arrows indicate fluxes with no data. To illustrate the magnitude of different fluxes, arrow size is proportional to the square root of corresponding flux.

302 **Discussion**

303 *ForC* v3.0 provided unprecedented coverage of most major variables, yielding an internally consistent picture
304 of C cycling in the world's major forest biomes. Carbon cycling rates generally increased from boreal to
305 tropical regions and with stand age. Specifically, the major C fluxes were highest in tropical forests,
306 intermediate in temperate (broadleaf or conifer) forests, and lowest in boreal forests – a pattern that generally
307 held for regrowth as well as mature forests (Figs. 6-7). In contrast to C fluxes, there was little directional
308 variation in mature forest C stocks across biomes (Figs. 2-5, 7). The majority of flux variables, together with
309 most live biomass pools, increased significantly with stand age (Figs. 6-11). Together, these results indicate
310 that, moving from cold to tropical climates and from young to old stands, there is a general acceleration of C
311 cycling, whereas C stocks and *NEP* of mature forests are correlated with a different set of factors.

312 **C variable coverage and budget closure**

313 The large number of C cycle variables covered by *ForC*, and the general consistency between them, provide
314 confidence that our overall reported means provide accurate and useful baselines for analysis (with the
315 caveats that they are unlikely to be accurate representations of C cycling for any particular forest, and that
316 these sample means almost certainly do not represent true biome means).

317 There are of course notable holes in the *ForC* variable coverage, as discussed by Anderson-Teixeira et
318 al. (xxxx), that limit the scope of our inferences here. Notably, *ForC* lacks coverage of fluxes to herbivores
319 and higher consumers, along with the woody mortality and dead wood stocks. Geographically, all variables
320 are poorly covered in Africa and Siberia, a common problem in the carbon-cycle community (Xu and Shang
321 2016 10.1016/j.jplph.2016.08.007, Schimel et al. 2015 10.1073/pnas.1407302112). *ForC* does not include soil
322 carbon, which is covered by other efforts (e.g. Köchy et al. 2015 10.5194/soil-1-351-2015). *ForC* is not
323 intended to replace databases that are specialized for particular parts of the C cycle analyses, e.g.,
324 aboveground biomass (REFS), land-atmosphere fluxes (Baldocchi et al. 2001
325 10.1175/1520-0477(2001)082<2415:FANTTS>2.3.CO;2), soil respiration (Jian et al. 2020
326 10.5194/essd-2020-136), or the human footprint in global forests (Magnani et al. 2007 10.1038/nature05847).

327 In this analysis, the C cycle budgets for mature forests (Figs. 2-5) generally “close”—that is, the sums of
328 component variables do not differ from the larger fluxes by more than one standard deviation. On the one
329 hand, this reflects the general fact that ecosystem-scale measurements tend to close the C budget more easily
330 and consistently than, for example, for energy balance (Stoy et al. 2013 10.1016/j.agrformet.2012.11.004). On
331 the other, however, as noted above *ForC* derives data from multiple heterogeneous sources, often with large
332 errors (standard deviations); as a result, the standard for C closure is relatively loose (cf Houghton 2020
333 10.1111/gcb.15050). Nonetheless, the lack of closure, in the few instances where it occurs, is probably more
334 reflective of differences in the representation of forest types (e.g., disproportionate representation of US
335 Pacific NW for aboveground woody biomass relative to AGB; Fig. 4) than of methodological accuracy. The
336 overall high degree of closure implies that *ForC* gives a consistent picture of C cycling within biomes. This is
337 an important and useful test, because it allows for consistency checks within the C cycle, for example
338 leveraging separate and independently-measured fluxes to constrain errors in another (Phillips et al. 2017
339 10.1007/s11104-016-3084-x, Williams et al. 2014 10.1016/j.rse.2013.10.034, Harmon et al. 2011
340 10.1029/2010JG001495), or producing internally consistent global data products (Wang et al. 2018
341 10.5194/gmd-11-3903-2018).

342 **C cycling across biomes**

343 Our analysis reveals a general deceleration of carbon cycling from the tropics to boreal regions. For mature
344 forests, this is consistent with a large body of previous work demonstrating that C fluxes generally decline
345 with latitude (or increase with temperature) on a global scale (e.g., ???, ???, Li and Xiao 2019, Banbury
346 Morgan *et al* n.d.). The consistency with which this occurs across numerous fluxes is not surprising, but has
347 never been simultaneously assessed across such a large number of variables (but see Banbury Morgan *et al*
348 n.d. for nine autotrophic fluxes). Thus, our analysis reveals that carbon cycling is most rapid in the tropics
349 and slowest in boreal regions, including C fluxes into (*GPP*), within (e.g., *NPP* and its components), and
350 out of (e.g., R_{soil} , R_{eco}) the ecosystem.

351 The notable exception to the pattern of fluxes decreasing from tropical to boreal regions is *NEP* (Fig. 6f),
352 which showed no significant differences across biomes. Unlike the other C flux variables, *NEP* does not
353 represent the rapidity with which C cycles through the ecosystem, but is the balance between C
354 sequestration (*GPP*) and respiratory losses (R_{eco}) and represents net CO₂ sequestration (or release) by the
355 ecosystem. *NEP* tends to be relatively small in mature forest stands [(???), **MORE REFS?**; discussed
356 further below], which accumulate carbon slowly relative to younger stands [(???)**; REFS**], if at all (**REFS**).
357 It is therefore unsurprising that there are no pronounced differences across biomes, suggesting that variation
358 in *NEP* of mature forests is controlled less by climate and more by other factors including moderate
359 disturbances (**REFS**) or disequilibrium of R_{soil} relative to C inputs [e.g., in peatlands where anoxic
360 conditions inhibit decomposition; **REFS**].

361 In contrast to the patterns observed for *NEP* in mature stands, *NEP* of stands between 20 and 100 years of
362 age varied across biomes, being lowest in boreal forests, intermediate in temperate broadleaf forests, and
363 highest in temperate conifer forests (with insufficient data to assess tropical forests; Figs. 6f, S1). This is
364 consistent with findings that live biomass accumulation rates (e.g., ΔB_{ag} or ΔB_{tot}) during early secondary
365 succession decrease with latitude [Anderson *et al* (2006); Cook-Patton *et al* (2020); Figs. 7a, S16-S22]. Note,
366 though, that *NEP* includes not only ΔB_{tot} , but also changes in DW_{tot} , *OL*, and soil carbon, and biome
367 differences in the accumulation rates of these variables have not been detected, in part because these variables
368 do not consistently increase with stand age [Cook-Patton *et al* (2020); Figs. 7, S23-S26; see discussion below].

369 For regrowth forests, little is known about cross-biome differences in carbon fluxes, and we are not aware of
370 any previous large-scale comparisons of C fluxes that have been limited to regrowth forests [although they're
371 commonly mixed in with mature forests; e.g., **REFS**]. Thus, this analysis was the first to examine flux
372 trends in regrowth forests across biomes. The observed tendency for young forest fluxes to decrease from
373 tropical to boreal regions paralleled patterns in mature forests (Figs. 6, S1-S15), suggesting that regrowth
374 forests follow latitudinal trends in carbon cycling similar to those of mature forests (e.g., Banbury Morgan *et*
375 *al* n.d.). Yet, *data remain sparse, and further work will be required to explore age x climate*
376 *interactions. Nevertheless, our broad-brush overview indicates that C cycling of regrowth forests is not only*
377 *higher in the tropics, parallel to fluxes in mature forests (Banbury Morgan et al n.d.), but also that it*
378 *accelerates more rapidly with stand age in the tropics, consistent with more rapid biomass accumulation.*

379 In contrast to C fluxes and biomass accumulation rates in regrowth forests, stocks showed less systematic
380 variation across biomes. For aboveground biomass, this Patterns are consistent with others studies showing
381 that variation in forest biomass across broad climatic gradients is modest and constrained more by moisture
382 than temperature (???). (???), using spaceborne lidar, showed a decline in aboveground biomass (all forests,

383 including secondary) with latitude in the N hemisphere, but values exceeding tropical forests in coastal
384 climates of both the southern and northern hemisphere. Highest biomass forests are found in temperate
385 oceanic climates (REF- , something in GEB, some global forest C map) (???). Lack of synthesis comparing
386 deadwood and organic layer across biomes, but see Cook-Patton *et al* (2020) for age trends.

387 Thus, biome differences should be interpreted more as driven more by geographic distribution of sampling
388 than by true differences.

389 **Age trends in C cycling**

390 (*Just some rough notes at this point*)

391 A relative dearth of data on C cycling in secondary forests, particularly in the tropics (Anderson-Teixeira et
392 al 2016), is problematic in that almost 2/3 of the world's forests were secondary as of 2010 (FAO 2010),
393 implying an under-filled need to characterize age-related trends in forest C cycling.

394 Moreover, as disturbances increase (???, McDowell *et al* 2020), understanding the carbon dynamics of
395 regrowth forests will be increasingly important.

396 It's also important to understand secondary forest C sequestration to reduce uncertainty regarding the
397 potential for carbon uptake by regrowth forests (???, Cook-Patton *et al* 2020).

398 (discuss NEP well, including) NEP increases with log(age) to 100 -> strongest C sinks are established
399 secondary forests. (But presumably this exact number is an artifact; don't over-emphasize.)

400 Our findings are largely consistent with, but built from a far larger dataset than, those of Pregitzer and
401 Euskirchen (2004 <http://dx.doi.org/10.1111/j.1365-2486.2004.00866.x>), who found that NPP and NEP to be
402 higher in intermediate-aged forests than older forests, and emphasize the importance of forest age at the
403 biome scale. Quickly-changing and age-dependent fluxes were also found in a number of previous syntheses
404 (Amiro *et al*. 2010 10.1029/2010JG001390, Magnani *et al*. 2007 10.1038/nature05847).

405 In contrast to most fluxes, *NEP* is highest at intermediate ages

406 **Relevance for climate change prediction and mitigation**

407 The future of forest C cycling (???) will shape trends in atmospheric CO₂ and the course of climate change.
408 For a human society seeking to understand and mitigate climate change, the data contained in *ForC* and
409 summarized here can help to meet two major challenges.

410 First, improved representation of forest C cycling in models is essential to improving predictions of the future
411 course of climate change. To ensure that models are giving the right answers for the right reasons, it is
412 important to benchmark against multiple components of the C cycle that are internally consistent with each
413 other. By making tens of thousands of records readily available in standardized format, *ForC* makes it
414 feasible for the modeling community to draw upon these data to benchmark models. Integration of *ForC*
415 with models is a goal (Fer *et al.*, in revision).

416 Second, *ForC* can serve as a pipeline through which forest science can inform forest-based climate change
417 mitigation efforts. Such efforts will be most effective when informed by the best available data, yet it is not
418 feasible for the individuals and organizations designing such efforts to sort through literature, often behind
419 paywalls, with data reported in varying units, terminology, etc. One goal for *ForC* is to serve as a pipeline

420 through which information can flow efficiently from forest researchers to decision-makers working to
421 implement forest conservation strategies at global, national, or landscape scales. This is already happening!
422 *ForC* has already contributed to updating the IPCC guidelines for carbon accounting in forests [IPCC 2019;
423 Requena Suarez *et al* (2019); Rozendaal *et al* in prep], mapping C accumulation potential from natural forest
424 regrowth globally (Cook-Patton *et al* 2020), and informing ecosystem conservation priorities (Goldstein *et al*
425 2020).

426 **ForC can complement remote sensing to provide a comprehensive picture of global forest C**
427 **cycling.** (*here, discuss what is well-covered by remote sensing, where ForC is useful for calibrating remote*
428 *sensing, and what ForC can get that remote sensing can't.*) AGB is the largest stock, and most of the
429 emphasis is on this variable. Remote sensing, with calibration based on high-quality ground-based data
430 (Schepaschenko *et al* 2019, Chave *et al* 2019), is the best approach for mapping forest carbon (REFS).
431 However, it is limited in that it is not associated with stand age and disturbance history, except in recent
432 decades when satellite data can be used to detect forest loss, gain, and some of their dominant drivers
433 (Hansen *et al* 2013, Song *et al* 2018, Curtis *et al* 2018). *ForC* is therefore valuable in defining age-based
434 trajectories in biomass, as in Cook-Patton *et al* (2020).

435 *Remote sensing measurements are increasingly useful for global- or regional-scale estimates of forest GPP*
436 *(???, Li and Xiao 2019), aboveground biomass (B_{ag}) (REFS), woody mortality (i.e., B_{ag} losses to mortality*
437 *M_{woody}) (Clark *et al* 2004, Leitold *et al* 2018), and to some extent net ecosystem exchange (NEP) (REFS).*
438 Other variables, in particular respiration fluxes, cannot be remotely sensed ((??)), and efforts such as the

439 Global Carbon Project (**le quere REF**) and NASA CMS (**citation:**

440 https://carbon.nasa.gov/pdfs/CMS_Phase-1_Report_Final_optimized.pdf but maybe
441 better to cite open literature, one of the papers listed at
442 <https://cmsflux.jpl.nasa.gov/get-data/publication-data-sets>) typically compute them as residuals
443 only. (**Ben, it woudl be particularly helpful if you could flesh this out some more.**)

444 In terms of C stocks, there is a paucity of data on dead wood and organic layer (Pan *et al.* ?). These can be
445 significant. (**Note that we've given a lot of emphasis to dead wood (work by Abby, and also**
446 **Jenny), and as a result this work really advances knowledge of dead wood. We'll want to**
447 **highlight that here.**) (*give some stats/ cite figures*).

448 **Move to data availability statement, or methods?**: We recommend that use of *ForC* data go to the
449 original database, as opposed to using “off-the-shelf” values from this publication. This is because (1) *ForC*
450 is constantly being updated, (2) analyses should be designed to match the application, (3) age equations
451 presented here all fit a single functional form that is not necessarily the best possible for all the variables.

452 As climate change accelerates, understanding and managing the carbon dynamics of forests will be critical to
453 forecasting, mitigation, and adaptation. The C data in *ForC*, as summarized here, will be valuable to these
454 efforts.

455 Acknowledgements

456 All researchers whose data is included in *ForC* and this analysis. Ian McGregor for help with the database.
457 Thanks to Norbert Kunert and [Helene's intern] for helpful input at an earlier phase. A Smithsonian
458 Scholarly Studies grant to KAT and HML. WLS grant to KAT.

459 **Data availability statement**

460 Materials required to fully reproduce these analyses, including data, R scripts, and image files, are archived
461 in Zenodo (DOI: TBD]. Data, scripts, and results presented here are also available through the open-access
462 *ForC* GitHub repository (<https://github.com/forc-db/ForC>), where many will be updated as the database
463 develops.

464 **ORCID iD**

465 Kristina J. Anderson-Teixeira: <https://orcid.org/0000-0001-8461-9713>

466 **References**

- 467 Anderson K J, Allen A P, Gillooly J F and Brown J H 2006 Temperature-dependence of biomass
468 accumulation rates during secondary succession *Ecology Letters* **9** 673–82 Online:
469 <http://www.blackwell-synergy.com/doi/abs/10.1111/j.1461-0248.2006.00914.x>
- 470 Anderson-Teixeira K, Herrmann V, CookPatton, Ferson A and Lister K 2020 Forc-db/GROA: Release with
471 Cook-Patton et al. 2020, Nature. Online: <https://zenodo.org/record/3983644>
- 472 Anderson-Teixeira K J, Davies S J, Bennett A C, Gonzalez-Akre E B, Muller-Landau H C, Joseph Wright S,
473 Abu Salim K, Almeyda Zambrano A M, Alonso A, Baltzer J L, Basset Y, Bourg N A, Broadbent E N,
474 Brockelman W Y, Bunyavejchewin S, Burslem D F R P, Butt N, Cao M, Cardenas D, Chuyong G B, Clay K,
475 Cordell S, Dattaraja H S, Deng X, Detto M, Du X, Duque A, Erikson D L, Ewango C E N, Fischer G A,
476 Fletcher C, Foster R B, Giardina C P, Gilbert G S, Gunatilleke N, Gunatilleke S, Hao Z, Hargrove W W,
477 Hart T B, Hau B C H, He F, Hoffman F M, Howe R W, Hubbell S P, Inman-Narahari F M, Jansen P A,
478 Jiang M, Johnson D J, Kanzaki M, Kassim A R, Kenfack D, Kibet S, Kinnaird M F, Korte L, Kral K,
479 Kumar J, Larson A J, Li Y, Li X, Liu S, Lum S K Y, Lutz J A, Ma K, Maddalena D M, Makana J-R, Malhi
480 Y, Marthews T, Mat Serudin R, McMahon S M, McShea W J, Memiaghe H R, Mi X, Mizuno T, Morecroft
481 M, Myers J A, Novotny V, Oliveira A A de, Ong P S, Orwig D A, Ostertag R, Ouden J den, Parker G G,
482 Phillips R P, Sack L, Sainge M N, Sang W, Sri-ngernyuang K, Sukumar R, Sun I-F, Sungpalee W, Suresh H
483 S, Tan S, Thomas S C, Thomas D W, Thompson J, Turner B L, Uriarte M, Valencia R, et al 2015
484 CTFS-ForestGEO: A worldwide network monitoring forests in an era of global change *Global Change Biology*
485 **21** 528–49 Online: <http://onlinelibrary.wiley.com/doi/10.1111/gcb.12712/abstract>
- 486 Anderson-Teixeira K J, Wang M M H, McGarvey J C, Herrmann V, Tepley A J, Bond-Lamberty B and
487 LeBauer D S 2018 ForC: A global database of forest carbon stocks and fluxes *Ecology* **99** 1507–7 Online:
488 <http://doi.wiley.com/10.1002/ecy.2229>
- 489 Anderson-Teixeira K J, Wang M M H, McGarvey J C and LeBauer D S 2016 Carbon dynamics of mature
490 and regrowth tropical forests derived from a pantropical database (TropForC-db) *Global Change Biology* **22**
491 1690–709 Online: <http://onlinelibrary.wiley.com/doi/10.1111/gcb.13226/abstract>
- 492 Baldocchi D, Falge E, Gu L, Olson R, Hollinger D, Running S, Anthoni P, Bernhofer C, Davis K, Evans R,
493 Fuentes J, Goldstein A, Katul G, Law B, Lee X, Malhi Y, Meyers T, Munger W, Oechel W, Paw K T,
494 Pilegaard K, Schmid H P, Valentini R, Verma S, Vesala T, Wilson K and Wofsy S 2001 FLUXNET: A New
495 Tool to Study the Temporal and Spatial Variability of Ecosystem-Scale Carbon Dioxide, Water Vapor, and

- 496 Energy Flux Densities *Bulletin of the American Meteorological Society* **82** 2415–34 Online:
497 [http://journals.ametsoc.org/doi/abs/10.1175/1520-0477\(2001\)082%3C2415:FANTTS%3E2.3.CO;2](http://journals.ametsoc.org/doi/abs/10.1175/1520-0477(2001)082%3C2415:FANTTS%3E2.3.CO;2)
- 498 Banbury Morgan B, Herrmann V, Kunert N, Bond-Lamberty B, Muller-Landau H C and Anderson-Teixeira
499 K J Global patterns of forest autotrophic carbon fluxes *Global Change Biology*
- 500 Bond-Lamberty B and Thomson A 2010 A global database of soil respiration data *Biogeosciences* **7** 1915–26
501 Online: <http://www.biogeosciences.net/7/1915/2010/>
- 502 Chave J, Davies S J, Phillips O L, Lewis S L, Sist P, Schepaschenko D, Armston J, Baker T R, Coomes D,
503 Disney M, Duncanson L, Héault B, Labrière N, Meyer V, Réjou-Méchain M, Scipal K and Saatchi S 2019
504 Ground Data are Essential for Biomass Remote Sensing Missions *Surveys in Geophysics* **40** 863–80 Online:
505 <https://doi.org/10.1007/s10712-019-09528-w>
- 506 Clark D B, Castro C S, Alvarado L D A and Read J M 2004 Quantifying mortality of tropical rain forest
507 trees using high-spatial-resolution satellite data *Ecology Letters* **7** 52–9 Online:
508 <https://onlinelibrary.wiley.com/doi/abs/10.1046/j.1461-0248.2003.00547.x>
- 509 Cook-Patton S C, Leavitt S M, Gibbs D, Harris N L, Lister K, Anderson-Teixeira K J, Briggs R D, Chazdon
510 R L, Crowther T W, Ellis P W, Griscom H P, Herrmann V, Holl K D, Houghton R A, Larrosa C, Lomax G,
511 Lucas R, Madsen P, Malhi Y, Paquette A, Parker J D, Paul K, Routh D, Roxburgh S, Saatchi S, Hoogen J
512 van den, Walker W S, Wheeler C E, Wood S A, Xu L and Griscom B W 2020 Mapping carbon accumulation
513 potential from global natural forest regrowth *Nature* **585** 545–50 Online:
514 <http://www.nature.com/articles/s41586-020-2686-x>
- 515 Curtis P G, Slay C M, Harris N L, Tyukavina A and Hansen M C 2018 Classifying drivers of global forest
516 loss *Science* **361** 1108–11 Online: <http://science.sciencemag.org/content/361/6407/1108>
- 517 Goldstein A, Turner W R, Spawn S A, Anderson-Teixeira K J, Cook-Patton S, Fargione J, Gibbs H K,
518 Griscom B, Hewson J H, Howard J F, Ledezma J C, Page S, Koh L P, Rockström J, Sanderman J and Hole
519 D G 2020 Protecting irrecoverable carbon in Earth's ecosystems *Nature Climate Change* 1–9 Online:
520 <http://www.nature.com/articles/s41558-020-0738-8>
- 521 Grassi G, House J, Dentener F, Federici S, Elzen M den and Penman J 2017 The key role of forests in
522 meeting climate targets requires science for credible mitigation *Nature Climate Change* **7** 220–6 Online:
523 <https://www.nature.com/articles/nclimate3227>
- 524 Griscom B W, Adams J, Ellis P W, Houghton R A, Lomax G, Miteva D A, Schlesinger W H, Shoch D,
525 Siikamäki J V, Smith P, Woodbury P, Zganjar C, Blackman A, Campari J, Conant R T, Delgado C, Elias P,
526 Gopalakrishna T, Hamsik M R, Herrero M, Kiesecker J, Landis E, Laestadius L, Leavitt S M, Minnemeyer S,
527 Polasky S, Potapov P, Putz F E, Sanderman J, Silvius M, Wollenberg E and Fargione J 2017 Natural climate
528 solutions *Proceedings of the National Academy of Sciences* **114** 11645–50 Online:
529 <http://www.pnas.org/lookup/doi/10.1073/pnas.1710465114>
- 530 Hansen M C, Potapov P V, Moore R, Hancher M, Turubanova S A, Tyukavina A, Thau D, Stehman S V,
531 Goetz S J, Loveland T R, Kommareddy A, Egorov A, Chini L, Justice C O and Townshend J R G 2013
532 High-Resolution Global Maps of 21st-Century Forest Cover Change *Science* **342** 850–3 Online:
533 <http://www.sciencemag.org/cgi/doi/10.1126/science.1244693>
- 534 Johnson D J, Needham J, Xu C, Massoud E C, Davies S J, Anderson-Teixeira K J, Bunyavejchewin S,

- 535 Chambers J Q, Chang-Yang C-H, Chiang J-M, Chuyong G B, Condit R, Cordell S, Fletcher C, Giardina C P,
 536 Giambelluca T W, Gunatilleke N, Gunatilleke S, Hsieh C-F, Hubbell S, Inman-Narahari F, Kassim A R,
 537 Katabuchi M, Kenfack D, Litton C M, Lum S, Mohamad M, Nasardin M, Ong P S, Ostertag R, Sack L,
 538 Swenson N G, Sun I F, Tan S, Thomas D W, Thompson J, Umaña M N, Uriarte M, Valencia R, Yap S,
 539 Zimmerman J, McDowell N G and McMahon S M 2018 Climate sensitive size-dependent survival in tropical
 540 trees *Nature Ecology & Evolution* **2** 1436–42 Online: <http://www.nature.com/articles/s41559-018-0626-z>
 541 Krause A, Pugh T A M, Bayer A D, Li W, Leung F, Bondeau A, Doelman J C, Humpenöder F, Anthoni P,
 542 Bodirsky B L, Ciais P, Müller C, Murray-Tortarolo G, Olin S, Popp A, Sitch S, Stehfest E and Arneth A
 543 2018 Large uncertainty in carbon uptake potential of land-based climate-change mitigation efforts *Global
 544 Change Biology* **24** 3025–38 Online: <https://onlinelibrary.wiley.com/doi/abs/10.1111/gcb.14144>
 545 Leitold V, Morton D C, Longo M, dos-Santos M N, Keller M and Scaranello M 2018 El Niño drought
 546 increased canopy turnover in Amazon forests *New Phytologist* **219** 959–71 Online:
 547 <http://doi.wiley.com/10.1111/nph.15110>
 548 Li X and Xiao J 2019 Mapping Photosynthesis Solely from Solar-Induced Chlorophyll Fluorescence: A
 549 Global, Fine-Resolution Dataset of Gross Primary Production Derived from OCO-2 *Remote Sensing* **11** 2563
 550 Online: <https://www.mdpi.com/2072-4292/11/21/2563>
 551 Lutz J A, Furniss T J, Johnson D J, Davies S J, Allen D, Alonso A, Anderson-Teixeira K J, Andrade A,
 552 Baltzer J, Becker K M L, Blomdahl E M, Bourg N A, Bunyavejchewin S, Burslem D F R P, Cansler C A,
 553 Cao K, Cao M, Cárdenas D, Chang L-W, Chao K-J, Chao W-C, Chiang J-M, Chu C, Chuyong G B, Clay K,
 554 Condit R, Cordell S, Dattaraja H S, Duque A, Ewango C E N, Fischer G A, Fletcher C, Freund J A,
 555 Giardina C, Germain S J, Gilbert G S, Hao Z, Hart T, Hau B C H, He F, Hector A, Howe R W, Hsieh C-F,
 556 Hu Y-H, Hubbell S P, Inman-Narahari F M, Itoh A, Janík D, Kassim A R, Kenfack D, Korte L, Král K,
 557 Larson A J, Li Y, Lin Y, Liu S, Lum S, Ma K, Makana J-R, Malhi Y, McMahon S M, McShea W J,
 558 Memiaghe H R, Mi X, Morecroft M, Musili P M, Myers J A, Novotny V, Oliveira A de, Ong P, Orwig D A,
 559 Ostertag R, Parker G G, Patankar R, Phillips R P, Reynolds G, Sack L, Song G-Z M, Su S-H, Sukumar R,
 560 Sun I-F, Suresh H S, Swanson M E, Tan S, Thomas D W, Thompson J, Uriarte M, Valencia R, Vicentini A,
 561 Vrška T, Wang X, Weiblen G D, Wolf A, Wu S-H, Xu H, Yamakura T, Yap S and Zimmerman J K 2018
 562 Global importance of large-diameter trees *Global Ecology and Biogeography* **27** 849–64 Online:
 563 <https://onlinelibrary.wiley.com/doi/abs/10.1111/geb.12747>
 564 Luyssaert S, Inglima I, Jung M, Richardson A D, Reichstein M, Papale D, Piao S L, Schulze E-D, Wingate L,
 565 Matteucci G, Aragao L, Aubinet M, Beer C, Bernhofer C, Black K G, Bonal D, Bonnefond J-M, Chambers J,
 566 Ciais P, Cook B, Davis K J, Dolman A J, Gielen B, Goulden M, Grace J, Granier A, Grelle A, Griffis T,
 567 Grünwald T, Guidolotti G, Hanson P J, Harding R, Hollinger D Y, Hutyra L R, Kolari P, Kruijt B, Kutsch
 568 W, Lagergren F, Laurila T, Law B E, Maire G L, Lindroth A, Loustau D, Malhi Y, Mateus J, Migliavacca M,
 569 Misson L, Montagnani L, Moncrieff J, Moors E, Munger J W, Nikinmaa E, Ollinger S V, Pita G, Rebmann
 570 C, Roupsard O, Saigusa N, Sanz M J, Seufert G, Sierra C, Smith M-L, Tang J, Valentini R, Vesala T and
 571 Janssens I A 2007 CO₂ balance of boreal, temperate, and tropical forests derived from a global database
 572 *Global Change Biology* **13** 2509–37 Online:
 573 <http://onlinelibrary.wiley.com/doi/abs/10.1111/j.1365-2486.2007.01439.x>
 574 McDowell N G, Allen C D, Anderson-Teixeira K, Aukema B H, Bond-Lamberty B, Chini L, Clark J S,
 575 Dietze M, Grossiord C, Hanbury-Brown A, Hurtt G C, Jackson R B, Johnson D J, Kueppers L, Lichstein J

- 576 W, Ogle K, Poulter B, Pugh T A M, Seidl R, Turner M G, Uriarte M, Walker A P and Xu C 2020 Pervasive
577 shifts in forest dynamics in a changing world *Science* **368** Online:
578 <https://science.sciencemag.org/content/368/6494/eaaz9463>
- 579 Pan Y, Birdsey R A, Fang J, Houghton R, Kauppi P E, Kurz W A, Phillips O L, Shvidenko A, Lewis S L,
580 Canadell J G, Ciais P, Jackson R B, Pacala S, McGuire A D, Piao S, Rautiainen A, Sitch S and Hayes D
581 2011 A Large and Persistent Carbon Sink in the World's Forests *Science* **333** 988–93 Online:
582 <http://www.sciencemag.org/content/early/2011/07/27/science.1201609.abstract>
- 583 Pugh T A M, Lindeskog M, Smith B, Poulter B, Arneth A, Haverd V and Calle L 2019 Role of forest
584 regrowth in global carbon sink dynamics *Proceedings of the National Academy of Sciences* **116** 4382–7
585 Online: <http://www.pnas.org/lookup/doi/10.1073/pnas.1810512116>
- 586 Requena Suarez D, Rozendaal D M A, Sy V D, Phillips O L, Alvarez-Dávila E, Anderson-Teixeira K,
587 Araujo-Murakami A, Arroyo L, Baker T R, Bongers F, Brienen R J W, Carter S, Cook-Patton S C,
588 Feldpausch T R, Griscom B W, Harris N, Héault B, Coronado E N H, Leavitt S M, Lewis S L, Marimon B
589 S, Mendoza A M, N'dja J K, N'Guessan A E, Poorter L, Qie L, Rutishauser E, Sist P, Sonké B, Sullivan M J
590 P, Vilanova E, Wang M M H, Martius C and Herold M 2019 Estimating aboveground net biomass change for
591 tropical and subtropical forests: Refinement of IPCC default rates using forest plot data *Global Change
592 Biology* **25** 3609–24 Online: <http://onlinelibrary.wiley.com/doi/abs/10.1111/gcb.14767>
- 593 Schepaschenko D, Chave J, Phillips O L, Lewis S L, Davies S J, Réjou-Méchain M, Sist P, Scipal K, Perger
594 C, Herault B, Labrière N, Hofhansl F, Affum-Baffoe K, Aleinikov A, Alonso A, Amani C, Araujo-Murakami
595 A, Armston J, Arroyo L, Ascarrunz N, Azevedo C, Baker T, Bałazy R, Bedeau C, Berry N, Bilous A M,
596 Bilous S Y, Bissiengou P, Blanc L, Bobkova K S, Braslavskaya T, Brienen R, Burslem D F R P, Condit R,
597 Cuni-Sánchez A, Danilina D, Torres D del C, Derroire G, Descroix L, Sotta E D, d'Oliveira M V N, Dresel C,
598 Erwin T, Evdokimenko M D, Falck J, Feldpausch T R, Foli E G, Foster R, Fritz S, Garcia-Abril A D,
599 Gornov A, Gornova M, Gothard-Bassébé E, Gourlet-Fleury S, Guedes M, Hamer K C, Susanty F H, Higuchi
600 N, Coronado E N H, Hubau W, Hubbell S, Ilstedt U, Ivanov V V, Kanashiro M, Karlsson A, Karminov V N,
601 Killeen T, Koffi J-C K, Konovalova M, Kraxner F, Krejza J, Krisnawati H, Krivobokov L V, Kuznetsov M A,
602 Lakyda I, Lakyda P I, Licona J C, Lucas R M, Lukina N, Lussetti D, Malhi Y, Manzanera J A, Marimon B,
603 Junior B H M, Martinez R V, Martynenko O V, Matsala M, Matyashuk R K, Mazzei L, Memiaghe H,
604 Mendoza C, Mendoza A M, Morozik O V, Mukhortova L, Musa S, Nazimova D I, Okuda T, Oliveira L C,
605 et al 2019 The Forest Observation System, building a global reference dataset for remote sensing of forest
606 biomass *Scientific Data* **6** 1–11 Online: <http://www.nature.com/articles/s41597-019-0196-1>
- 607 Song X-P, Hansen M C, Stehman S V, Potapov P V, Tyukavina A, Vermote E F and Townshend J R 2018
608 Global land change from 1982 to 2016 *Nature* **560** 639–43 Online:
609 <http://www.nature.com/articles/s41586-018-0411-9/>
- 610 Taylor P G, Cleveland C C, Wieder W R, Sullivan B W, Doughty C E, Dobrowski S Z and Townsend A R
611 2017 Temperature and rainfall interact to control carbon cycling in tropical forests ed L Liu *Ecology Letters*
612 **20** 779–88 Online: <http://doi.wiley.com/10.1111/ele.12765>